Materials Today Bio 3 (2019) 100024

Contents lists available at ScienceDirect

Materials Today Bio

journal homepage: www.journals.elsevier.com/materials-today-bio

Three-dimensional printing of metals for biomedical applications

J. Ni [a,b,c,e,l], H. Ling [b,c,d,l], S. Zhang [a,b,c,**,l], Z. Wang [a,b,c], Z. Peng [f], C. Benyshek [a,b,c], R. Zan [e], A.K. Miri [a,b,c], Z. Li [a,b,c,g], X. Zhang [e], J. Lee [a,b,c], K.-J. Lee [a,b,c], H.-J. Kim [a,b,c], P. Tebon [a,b,c], T. Hoffman [a,b,c], M.R. Dokmeci [a,b,c,h], N. Ashammakhi [a,b,c,h], X. Li [d,i], A. Khademhosseini [a,b,c,h,j,k,*]

[a] Department of Bioengineering, University of California-Los Angeles, Los Angeles, CA 90095, USA
[b] Center for Minimally Invasive Therapeutics (C-MIT), University of California-Los Angeles, Los Angeles, CA 90095, USA
[c] California NanoSystems Institute, University of California-Los Angeles, Los Angeles, CA 90095, USA
[d] Department of Mechanical and Aerospace Engineering, University of California-Los Angeles, Los Angeles, CA 90095, USA
[e] State Key Laboratory of Metal Matrix Composites, School of Materials Science and Engineering, Shanghai Jiao Tong University, Shanghai 200240, PR China
[f] Department of Orthopaedic Surgery, Ningbo Medical Treatment Center Lihuili Hospital, PR China
[g] School of Mechanical Engineering, Xi'an Jiaotong University, Xi'an, 710049, China
[h] Department of Radiology, David Geffen School of Medicine, University of California-Los Angeles, Los Angeles, CA 90095, USA
[i] Department of Materials Science and Engineering, University of California-Los Angeles, Los Angeles, CA 90095, USA
[j] Department of Chemical and Biomolecular Engineering, University of California-Los Angeles, Los Angeles, CA 90095, USA
[k] Department of Bioindustrial Technologies, College of Animal Bioscience and Technology, Konkuk University, Seoul, Republic of Korea

ARTICLE INFO

Keywords:
3D printing
Biometals
Biocompatibility
Medical devices
Clinical application

ABSTRACT

Three-dimensional (3D) printing technology has received great attention in the past decades in both academia and industry because of its advantages such as customized fabrication, low manufacturing cost, unprecedented capability for complex geometry, and short fabrication period. 3D printing of metals with controllable structures represents a state-of-the-art technology that enables the development of metallic implants for biomedical applications. This review discusses currently existing 3D printing techniques and their applications in developing metallic medical implants and devices. Perspective about the current challenges and future directions for development of this technology is also presented.

1. Introduction

People of age 65 or older are now accounting for nearly 10% of the world's population, and this number is expected to double by the year of 2050 [1]. These senior people are more likely to experience health complications such as bone fractures and tissue loss due to their age. Solving these complications then requires fixation, reconstruction, or replacement. Because of the mechanical demands of hard tissue, metals are usually used to provide support, enable immediate mobilization of patients, and prevent the development of complications [2,3]. Currently, approximately 70–80% of the clinically used implants are made of stainless steels [4], cobalt-chromium alloys [5], titanium alloys [6,7], nitinol [8,9], tantalum [10,11], and niobium [12,13]. More recently, there has been an increasing interest to study biodegradable metals including magnesium [14], iron [15], zinc [16–18], and calcium [19], and many new findings have been reported over the last decade [14,20,21].

As an advanced manufacturing technology that integrates light, machinery, electricity, computers, digital control, and new materials, 3D printing is gradually adopted in almost all industries, triggering a revolution in manufacturing [22,23]. Today, it has been widely applied in the biomedical fields, not only for the repair of human tissues [24], such as orthopedic and dental implants, artificial livers, and artificial cardiovascular systems [25], but also for microfluidic devices [26,27] and medical electronics [28].

Owing to mismatch of mechanical properties between metallic implants and bone, stress shielding is prone to appear, leading to consequent bone resorption and eventual implantation failure. Thus, new

* Corresponding author. Department of Bioengineering, University of California-Los Angeles, Los Angeles, CA 90095, USA.
** Corresponding author. Department of Bioengineering, University of California-Los Angeles, Los Angeles, CA 90095, USA.
E-mail addresses: zhangshiming@ucla.edu (S. Zhang), khademh@ucla.edu (A. Khademhosseini).
[l] These authors contributed equally to this work.

https://doi.org/10.1016/j.mtbio.2019.100024
Received 12 May 2019; Received in revised form 8 August 2019; Accepted 12 August 2019
Available online 20 August 2019

methods to develop biomimetic devices are necessary. Complex external shapes and intricate internal architecture are difficult to obtain using conventional casting and powder metallurgy methods. However, with the development of 3D printing, it is possible to print metallic implants with controlled porosity and a modulus matching closely to that of the native bone, thereby reducing problems related to stress shielding [29]. The mass production of these metallic implants is also enabled because 3D printing has benefits of low cost, short manufacturing period, and high repeatability. Moreover, this technology is integrated with computer-aided design (CAD) technique, allowing for customized models designed with high degree of freedom. As a result, 3D printing offers the unprecedented possibility to advance personalized medicine by developing custom-made metallic implants that can fit specific tissue defects [30]. Therefore, significant efforts have been made to develop implants that can closely resemble native bone structural and functional properties.

The rapid development of this technology has allowed for the emergence of alternative 3D printing methods, which overcome the disadvantages of the commonly used laser and electron beam printing. At present, 3D printed biometals are mainly used to produce implants for tissue repair, dentistry and orthopedics, and surgical tools (Fig. 1). In the future, the development of 3D printed biodegradable metals and liquid metals will further extend to new biometal applications, such as implantable and/or biodegradable, metal bioelectronics. The present paper reviews the applications of biometals fabricated by traditional 3D printing technology and the new implications derived from emerging 3D printing technology.

2. Metal 3D printing techniques for biomedical applications

Additive manufacturing methods give rise to the mass fabrication of metallic implants with complex geometry and internal structures as well as the production of customized medical implants that meet specific individual needs, thus becoming very promising for clinical applications [39]. For example, by adopting 3D printing technique, mass production of accurate anatomic models can be achieved, and orthopedic surgeons could use them for operation preparation. In addition, patient-specific implants can be obtained with 3D printing by establishing CAD models based on patients' X-ray computed tomography (X-ray CT) or magnetic resonance imaging (MRI). Thus, 3D printing techniques may be very suitable for the fabrication of medical devices using biometals. The current commonly used 3D printing techniques for biometals are introduced in this section, and a summary of 3D metal printing methods is shown in Table 1 [40–46].

2.1. Selective laser sintering

Selective laser sintering (SLS) was first proposed and then patented in 1989 [47]. In this process, liquid-phase sintering is used as the metallurgical mechanism. The powder material during the forming process is partially melted, retaining its solid phase core, and powder densification is achieved by subsequent solid-phase particle rearrangement and liquid-phase solidification bonding [48,49]. The commonly used device in SLS consists of a powder cylinder and a forming cylinder. The piston of the powder cylinder rises, and the material powder is evenly layered on

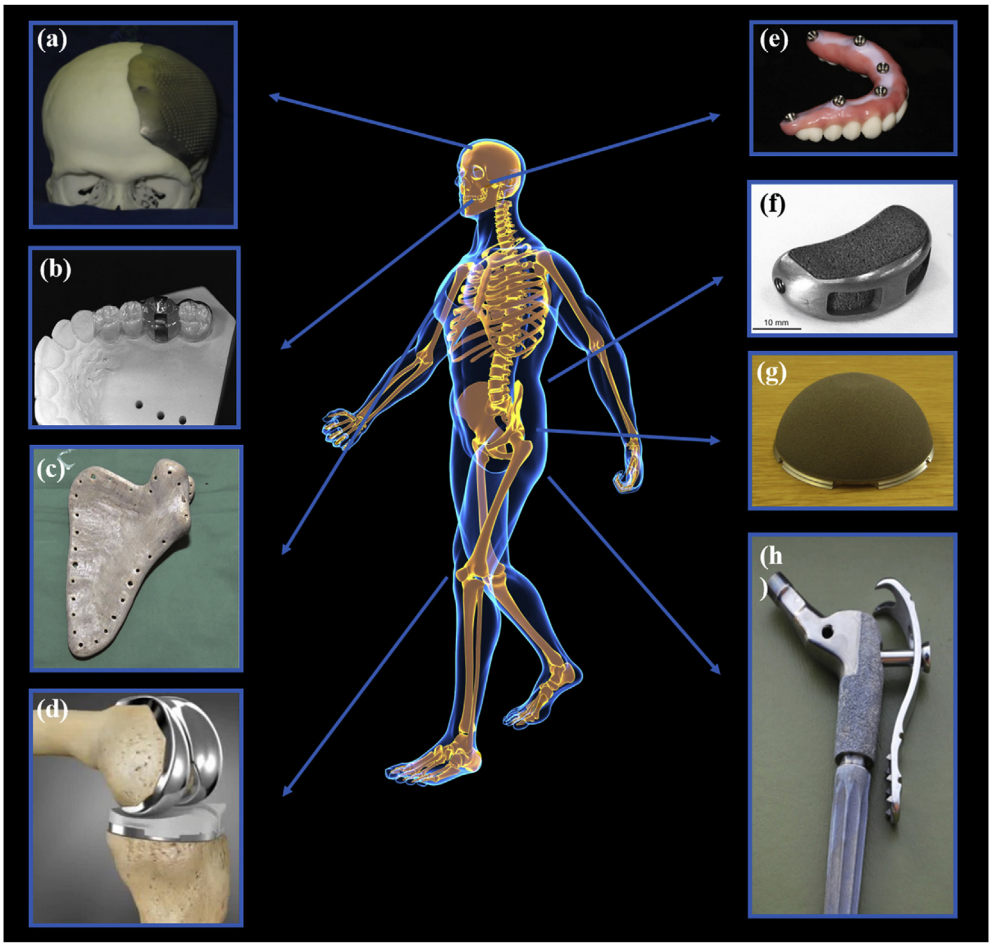

Fig. 1. The biomedical application of 3D printing of biometals includes (a) cranial prosthesis [31]; (b) surgical guide [32]; (c) scapula prosthesis [33]; (d) knee prosthesis [34]; (e) dental implants [35]; (f) interbody fusion cage [36]; (g) acetabular cup [37]; and (h) hip prosthesis [38]. Reprint with permission.

Table 1
Summary of 3D printing methods for biometals.

Technique name	Applicable metals	Processing parameters	Advantages	Limitations
Selective laser sintering (SLS)	Ti alloys; cobalt-chromium; stainless steel; Ni–Ti alloy	Laser sintering; powder;	1. A great variety of printable materials	1. Porous internal structure and rough surface finish, requiring postprinting process
		An inert environment (Ar or N2);	2. High utilization (unsintered powder can be removed and reused)	2. Printable precision is limited by the size of particles of the used materials
		CO2 laser (9.2–10.8 μm);	3. No requirement for support for printing of overhanging structure	
		Scan strategy: unidirectional and bidirectional fills		
Selective laser melting (SLM)	Almost all metal alloys	Laser melting; powder (size: 10–45 μm)	1. Ability to tune properties of fabricated during printing process	1. Expensive
		An inert environment (Ar or N2);	2. Relatively low direct cost	2. Relatively slow process due to printing speed limitation compared with traditional machining
		Nd-YAG laser (1.064 μm)/fiber laser (1.09 μm);	3. Comprehensive functionality including reduced assembly time, improve material utilization, etc.	3. Acute size restriction
		Scan strategy: unidirectional and bidirectional fills/island scanning/contour melting	4. Good mechanical properties and low surface roughness for fabricated parts	
Laser direct metal deposition (LDMD)	Almost all metal alloys	Laser melting; powder (size: 20–200 μm);	1. Localized heat input and consequently low distortion, allowing printing of metal with high melting point	1. Low dimensional accuracy
		An inert environment (Ar or N2);	2. Fabrication of near net–shaped parts	
		Nd-YAG laser (1.064 μm);	3. Fabricate functional gradient materials and parts	2. Poor surface roughness
		scan strategy: unidirectional and bidirectional fills		
Selective electron beam melting (SEBM)	Almost all metal alloys	Electron beam melting;	1. High density for printed parts	1. Requires vacuum environment
		Power (size: 45–106 μm);	2. High product strength and less impurity due to vacuum melting	2. Poor surface finish and requires postprinting process
		Vacuum-capable chamber and a small quantity of He for reducing electrical charging;	3. Fabrication of brittle materials due to reduced cooling rate	3. Expensive equipment
		Scan strategy: unidirectional and bidirectional fills/spot mode	4. Multiple parts can be produced simultaneously	4. Low dimensional accuracy of parts
Laser-induced forward transfer (LIFT)	Chromium, tungsten, gold, nickel, aluminum	Pulse laser/layer	1. Very small-scale part processing	1. Small-batch production
			2. Easy operation and without vacuum environment or cleanroom	2. Small size and thin layers
			3. Wide range of printed materials	3. Weak structural support
			4. High accuracy (several μm)	
Atomic diffusion additive manufacturing (ADAM)	Sinterable metal powder: stainless steel, Ti alloys	Metal powder wrapped in plastic binder	1. The density of parts can reach about 95–99%	Longer lead time to strong part
			2. Low cost	
			3. High-quality surface	
			4. Precise complex structure	
			5. Excellent isotropic performance	
			6. Batch production	
Nanoparticle jetting (NPJ)	Ti alloys	A common inkjet nozzle/metal nanoparticles wrapped in liquid ink	1. High speed	Temperature tolerance of product is lower than that of those produced by traditional metal 3D printing
			2. Low cost	
			3. Simple and safe operation	
			4. High resolution (1 μm)	
			5. High precision and surface finish	
Inkjet 3D printing (3DP)/ binder jetting	Ti alloys	A fine water jet/metal powder	1. Low cost	Low precision
			2. Simple and safe operation	

the forming cylinder's piston (working piston) by the powdering roller. A computer controls a two-dimensional (2D) scanning trajectory of a laser beam according to the prototype slicing model to selectively sinter the solid powder material, forming a layer of the sample. After completing one layer, the working piston goes down by one layer's thickness, new powder is layered, and the laser beam scans the new layer. This cycle repeats, and layers are stacked until the desired 3D sample forms. The SLS process adopts a semisolid liquid–phase sintering mechanism, so the powder does not completely melt. Although the thermal stress accumulated by the forming material can be reduced to some extent, the formed portion contains solid-phase particles, which directly leads to high porosity and density. This can cause process defects such as low tensile strength and poor surface roughness. Still, SLS is advantageous because of the large selection of molding materials and simplicity of the molding process (no support is required) [50,51].

2.2. Selective laser melting

The idea of selective laser melting (SLM) was first proposed in 1995 [49]. This technology is developed based on SLS, and thus, the basic principles of the two are similar. SLM uses advanced high-energy fiber lasers, high-precision paving powder, and metallurgical mechanisms that completely melt powders for the rapid laser prototyping of metal components (Fig. 2a) [52]. The process of the SLM is carried out in a vacuum or inert gas–protected chamber to prevent the metal from reacting with other gases at elevated temperatures. SLM directly manufactures functional metal parts without intermediate processes. The higher laser energy density and finer focusing spot produce functional parts with higher dimensional accuracy and better surface roughness. Because the metal powder is completely melted, formed metal parts have metallurgically bonded structures, high densities, and good mechanical properties and

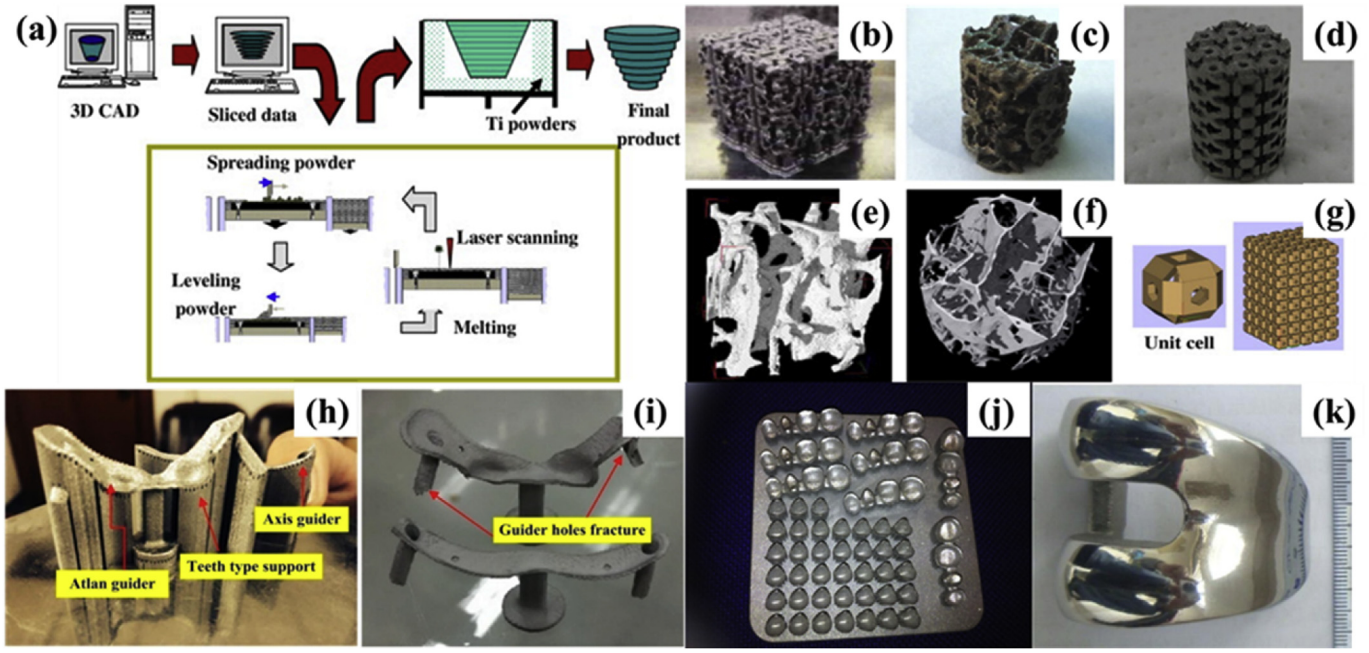

Fig. 2. (a) Processing flowchart of SLM; (b)–(d) 3D printed titanium porous structures prepared by SLM; (e)–(f) Micro-CT images of human cancellous bones; (g) stacked hollow cubes [52]; a spinal surgery template obtained by SLM; (h) the surgical template with its support; (i) the surgical template after abrasive blasting [55]; (j) the dental restorations made by SLM system [56]; (k) the lateral surface of a personalized femoral component after hand polishing [57]. Reprint with permission. CAD, computer-aided design; SLM, selective laser melting; CT, computed tomography.

does not required post-treatments [53,54]. The powder material can be a single or multicomponent substance, and the raw materials need not be specially prepared. SLM can significantly shorten the manufacturing period and reduce the cost of parts, while offering the advantage of design freedom. A wide choice of materials can be fabricated by SLM, while reducing the waste of materials. Functional parts with complex geometries can be prepared directly by SLM, making it especially suitable for single-piece or small-volume parts manufacturing.

In recent years, SLM has become a research hotspot and major development trend of rapid prototyping [58]. This technique can print a great variety of materials, including metals [59], polymers [60], metal combinations [49], metal-polymer combinations [61], and metal-ceramic combinations [49]. Almost any shape of fully metallurgical, high-precision, and near-density metal parts can be produced by SLM. As a result, this technique is used widely in medical applications to form complex-structure implants (Fig. 2b–g) [52] with sufficient biocompatibility, such as personalized orthopedic surgery templates (Fig. 2h and I) [55], dental restorations (Fig. 2j) [56], and femoral implants (Fig. 2k) [57]. The SLM technique has been widely used to process medical metals, such as stainless steel, titanium alloys, nickel-based superalloys, and cobalt-based alloys. SLM can produce geometrically complex parts with high dimensional accuracy and good surface state. No subsequent processing is required, which is needed during conventional processes (e.g. casting and machining). Because of these, SLM has become an ideal method to fabricate complex or functional gradient structures with accurate dimensions. This encourages its use for the preparation of metallic implants and scaffolds [62], including internal or surface porous structures for osseointegration between the bones and the implant [63]. SLM 3D printing is evolving into a powerful additive manufacturing technique for the processing of personalized, complicated biometallic devices [64,65].

2.3. Laser direct metal deposition

Laser direct metal deposition (LDMD) was first proposed by the Sandia National Laboratory in the 1990s and has since been further developed in many parts of the world [66]. Many universities and institutions have studied LDMD independently, resulting in the various names for this technique such as laser-engineered net shaping (LENS), directed metal deposition (DMD), laser rapid forming (LRF), and so on. Although they differ in name, their basic principle is the same. During the molding process, a nozzle aggregates powder on its working plane, while its laser beam centers to a point. The laser solidifies the powder which it shines on, creating a stacked entity at that position (Fig. 3a and b) [67,68]. While SLS/SLM is processed on a powder, LDMD is different in that it delivers metal powder through a nozzle. It is advantageous because if its abilities to make large volume parts and mix different kinds of metal powder within its nozzle to create specific metal alloys. In addition to manufacturing complete parts, LDMD's typical applications include repairing, coating, and adding feature structures. LDMD has the potential to fabricate structures with gradients of pores or gradients of different metals, including titanium alloys [69], stainless steels, and shape memory alloys that have greater geometric flexibility compared with materials printed by other techniques [70]. Xue et al. [72] fabricated net shape porous titanium (Fig. 3c) [71] by LENS for load-bearing bone. The porous titanium implant possessed a Young's modulus range from 2.6 to 44 GPa and mechanical strength from 24 to 463 MPa, which are closer to the mechanical properties of natural bones than dense titanium. Through *in vitro* testing, the porous titanium demonstrated enhanced cell adhesion and proliferation that allowed cell growth into the pores, with an optimal size greater than 200 μm. Bandyopahdyay et al. [73] fabricated porous Ti6Al4V alloy samples (Fig. 3d) using LENS, whose in vivo results in male Sprague-Dawley rats for 16 weeks showed significantly increased calcium content inside the implant, which indicated that biological tissue could grow into the implant through the interconnected pores. Moreover, this study also confirmed that tissue ingrowth is largely determined by the total amount of pores in the implant.

Owing to the large laser focusing spot, the precision of LDMD is generally above 1 mm. Although a dense metal entity with metallurgical bonding can be obtained, its dimensional accuracy and surface finish are not very desirable, and further machine processing is needed before actual use. Owing to the layer-additive feature of LDMD, the deposited material repeatedly undergoes complex thermal cycling processes in different regions, which involves melting and numerous reheat cycles at

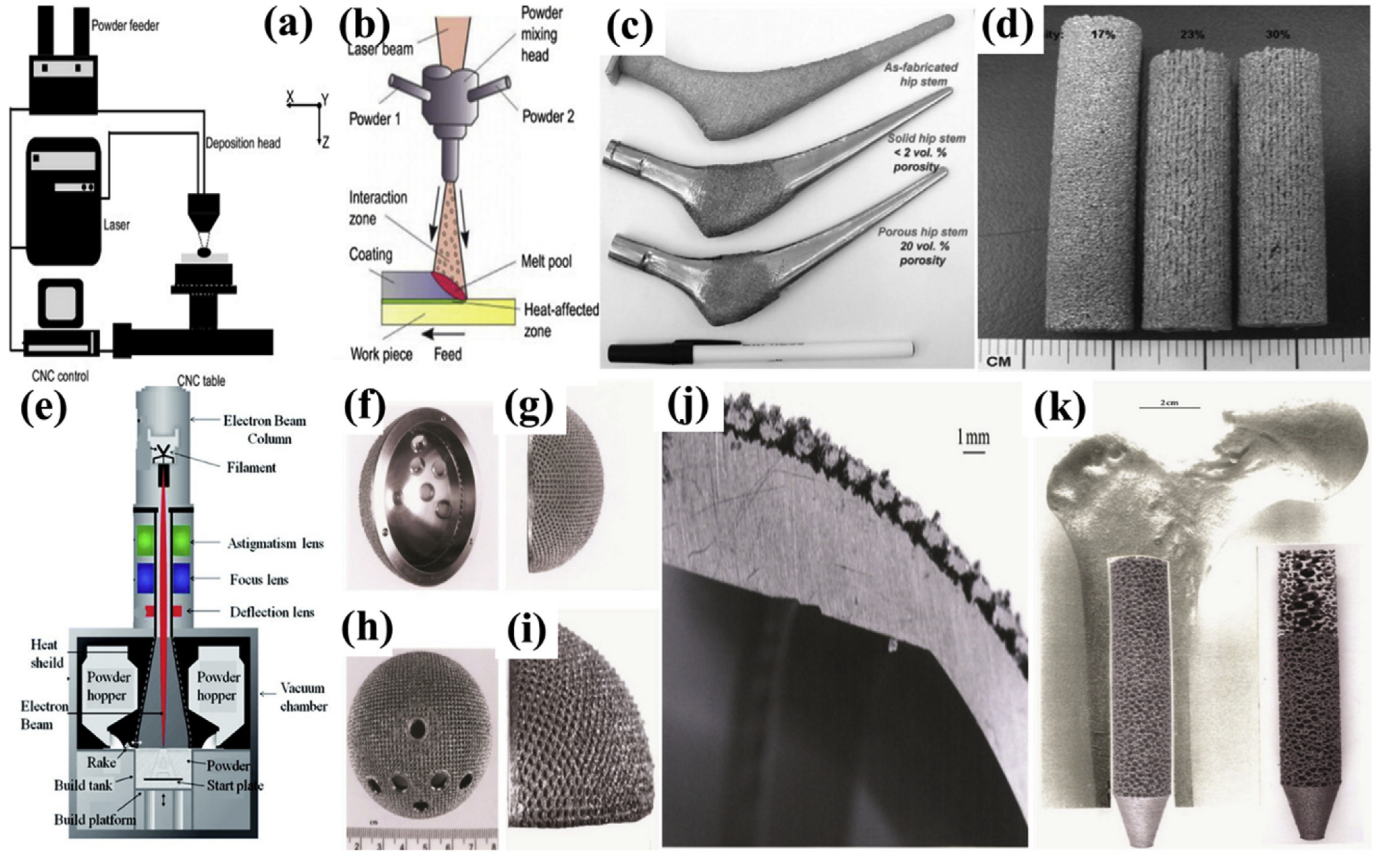

Fig. 3. (a), (b) Schematic depictions of the LDMD process [67,68]; (c) LENS-produced functional hip stems with different porosity: 0% porosity, <2 vol% porosity, and 20 vol% porosity [71]; (d) typical porous Ti6Al4V samples fabricated by LDMD [73]; (e) schematic depiction of the SEBM technique [75]; (f)–(j) a Ti–6Al–4V acetabular cup fabricated by SEBM with outer porous mesh structure enabling ingrowth of hip bones: (f), (g) lateral views; (h), (i) local magnification of the outer porous mesh structure; (j) sectional view of the acetabular cup; (k) a SEBM-fabricated Ti–6Al–4V simulated intramedullary rod insert [76]. Reprint with permission. LENS, laser-engineered net shaping; LDMD, laser direct metal deposition; SEBM, selective electron beam melting; CNC, computer numeric control.

lower temperatures, and this thermal behavior leads to complex phase transitions and microstructure changes. Therefore, it is difficult to control the composition and structure required for desired parts. Still, the rapid formation of a molten pool from the fine laser beam leads to melting instability and a faster solidification rate. Complex residual stresses are easily generated because of the transient changes in heat during the part's solidification, and the presence of residual stress inevitably leads to the occurrence of deformation or cracks in the LDMD-shaped parts. The uncontrollability of composition and microstructure and the formation of residual stress are the two major drawbacks of LDMD technology [74].

The mechanical properties of metallic parts prepared by laser-processed 3D printing technology, which commonly uses high-energy laser sources to heat and melt raw metal materials (powder, wire) and layer stack, can reach that of metal parts produced by the traditional manufacturing process. However, owing to the point-by-point scanning and stacking of laser or electron beams, materials will undergo rapid heating and cooling in the process of part forming, resulting in a high temperature gradient and inevitably producing complex residual stress distribution, which causes the cracks and deformation of metal parts [40,77]. This high residual stress will also affect the mechanical properties and corrosion resistance [77]. The current methods of reducing or eliminating residual stresses include the following [78,79]: (a) optimum design: residual stress should be considered to avoid in the design process; (b) change of laser scanning mode: the laser scanning vector is rotated from one processing layer to the next, preventing the stress from concentrating on the same plane; (c) avoiding large area and uninterrupted sintering; and (d) preheating powder bed and stress removal annealing for metal parts.

2.4. Selective electron beam melting

Similar to SLS and SLM, selective electron beam melting (SEBM) is a rapid manufacturing technique that uses high-energy, high-speed electron beams to selectively bombard metal powders, melting the powder material and forming 3D samples. The process of SEBM is as follows: first, a layer of powder is spread on the paving plane; then, the electron beam is selectively aligned to these powders according to the cross-sectional profile information of a 3D CAD file from the computer; next, the metal powder is melted layer-by-layer, bonding with the formed part below by a magnetically directed electron beam (up to 3 kW power) in a high-vacuum atmosphere until the entire part is completed; finally, the excess powder is removed to obtain the desired 3D sample (Fig. 3e) [75]. Presently, a lot of research is being conducted to find the influences of the process parameters such as the electron beam current, focusing current, action time, powder thickness, acceleration voltage, and scanning mode [50,80]. SEBM uses a high-energy electron beam as a processing heat source that scans by manipulating a magnetic deflection coil without mechanical inertia. In addition, the vacuum environment can prevent the metal powder from being oxidized during liquid-phase sintering or melting. Compared with lasers, the electron beam has the advantages of a high energy utilization rate, a high material absorption rate, better stability, and low operation and maintenance costs. Compared with other methods, SEBM technology has higher efficiency, smaller part deformation, no support for the molding process, and denser microstructure formation. The faster and more sensitive deflection focus control of the electron beam is controlled by a magnetic field, which allows the deflection and focus length of the beam to be quickly and sensitively

manipulated by changing the intensity and direction of the electrical signal. Furthermore, although the electron beam deflection focusing system is not disturbed by metal evaporation, it is difficult to achieve high dimensional accuracy and a fine structure for the molded portion because of the inability of electron beam to focus on a fine spot [81].

SEBM is one of the most common 3D printing techniques applied for biometallic devices [82,83], such as acetabular cups with outer porous mesh structure regions (Fig. 3f–j) [76], Co–29Cr–6Mo alloy femoral knee implants, and intramedullary rods (Fig. 3k) [76]. However, the optimization of the implant surface finish, which are largely dependent on SEBM parameters, such as powder size beam flow and part orientation, are a challenge of using this technique for orthopedic implants [84].

Presently, mainstream biometal 3D printing uses laser or electron beams as heat sources and metal powder as the material. The processing parameters (chamber atmosphere, scan strategy, feedstock, powder type, etc) affect significantly the quality of 3D printed metal parts (feature size, surface roughness, density, porosity, etc) [40]. For example, the diameter of the heat source and the size of the feedstock determine the feature size, thus the minimum feature size of SLM is lower than that of EBM [85]. Meanwhile, SLM-printed metal parts have less surface roughness than that of EBM-printed parts because SLM can manufacture finer powder [86]. In addition, process temperature of these techniques also causes some common defects (residual stress, delamination, cracking, swelling, etc). Cracks also appear when molten metal solidifies or further heated. Inadequate melting of feedstock or remelting of several layers beneath the molten pool cause layer delamination, resulting in the interlayer fracture [40].

Printing is an expensive process, from the high cost of both metal powder and devices, which can be millions. With increasing interest in the use of metal 3D printing for manufacturing, more capital and scientific research have been aimed at improving the technology and reducing the cost. Although not yet commercially available, some of these efforts provide great potential using new methods that can inspire new ideas for the industry.

2.5. Laser-induced forward transfer

In most cases, metal printing is limited to materials with lower melting points. So far, it has proven to be either very difficult or extremely expensive to 3D print metals such as copper or gold. It is for this reason that laser-induced forward transfer (LIFT) was developed. LIFT is a direct printing method which can deposit a wide range of metals after laser interactions [87]. This technique does not require metal powder, and its working principle is different from conventional metal 3D printing technologies. A focused, pulsed laser is exposed onto a thin layer of metal material, called the 'donor film,' resulting in a thermal stress wave or evaporation that subsequently yields the ejection of a liquid micron-sized droplet onto a transparent substrate (known as the receiver). Following impact, the droplet cools down and solidifies [88]. LIFT has been developing throughout the years, and some improvements to the original approach have been introduced (Fig. 4a) [89]. This method has been successfully applied to printing chromium [90], gold [91], titanium [89], nickel [92], and aluminum [93]. Thick metal printing by LIFT suffers from low aspect ratio pillars because of the lack of good adhesion between stacked droplets. The deposited droplets are solidified into a sphere-like shape, which reduces the contact/adhesion surface between two subsequent layers, and the relatively large distances between donor and receiver hampers the precision of layer-by-layer deposition. LIFT can accurately print vertical wires, but it cannot generate overhang and large 3D constructs [94]. These geometric limitations come from the nature of LIFT, which may require sacrificial support materials. LIFT can be used to fabricate biosensors [89]. As an example, LIFT was recently used to print small scale objects with a copper/silver alloy on a copper sacrificial support [95]. In terms of resolution, reported LIFT metal structures have lateral dimensions of several micrometers [96]; the smallest size is nearly 3 μm [97]. Recently, the LIFT method was used to print a very small (2 mm high and 5 μm diameter) 3D tower using copper and gold as the raw materials. Disc-like droplets were also demonstrated using low-energy lasers for better layer stacking and bonding (Fig. 4b) [97].

2.6. Atomic diffusion additive manufacturing

In recent years, atomic diffusion additive manufacturing (ADAM) has been introduced as a new 3D printing method to print metal powders wrapped in plastic binders layer-by-layer [99]. The plastic binder can be removed in a sintering furnace after printing, and the metal powder is sintered with a density of 95–99%. The process of sintering the entire component at one time promotes the growth of metal crystals through its adhesive layer, which efficiently eliminates the problem of low interlayer strength evident in other 3D printing processes. In addition, at a maximum printing size of 250 mm × 220 mm x 200 mm, the ADAM printer can print geometrical dimensions beyond other metal 3D printing methods. Also, it provides online process laser detection based on its cloud software. Users can check each printing layer and monitor it through the software. The printer integrates a metal material handling system with a remote access method via the cloud. 17-4 and 303 stainless steel can be molded by the printer in 3D, and compatibility with Ti6Al4V and A-2 and D-2 steels is being investigated. Compared with traditional metal 3D printing techniques, the main advantages of ADAM are as follows: it is 100 times faster than the traditional machining method, is one-tenth the cost of traditional metal 3D printing, produces part surfaces of high quality without post treatment, creates precise, complex structures, enables excellent isotropic performance, and is suitable for batch production.

2.7. Nanoparticle jetting

As a newly developed 3D printing technology for metal, nanoparticle jetting (NPJ) came out in 2016. As opposed to the conventional metal 3D printing technology that uses metal powder particles, this method uses liquid ink that wraps metal powders [99]. To obtain these, large metal pieces are crushed into nanoparticles, and the nanoparticles are injected into a binder to form a uniform printing ink [99]. Within the ink, the metal particles are uniformly distributed in a suspended state, and once suspended properly, the ink is ejected through a nozzle to enable layer-by-layer printing. Using ink this way is beneficial because it makes the entire product smoother. A common inkjet printhead can be used as a deposition tool in the printing process. After printing, the chamber evaporates excess binder by heating, leaving only the metal portion. This process can reach resolutions of 1-μm thickness, and its forming temperature is only about 300 °C. The technology can deposit 221 million droplets of ink per second, making NPJ 5 times faster than ordinary laser printing. NPJ reduces the material waste, saves costs, and can create almost any complex shape. The parts have high precision and surface finish, and NPJ has simpler and safer operation procedures. The disadvantage of this method is that the temperature tolerance of product is lower than traditional metal 3D printing. Still, NPJ is a novel technology that provides a simple and clean operation without the need to design and remove complex support structures.

2.8. Inkjet 3DP/binder jetting

A fine water jet is printed accurately, layer-by-layer, by an ink cartridge onto a metallic powder bed, under the control of the CAD file (Fig. 4c) [98]. Then the printed metal parts are subsequently sintered in a furnace to achieve the required mechanical strength. This technique does not use laser or electron beam to melt the metallic powders, as mainstream 3D metal printing technology does. The main advantages of Inkjet 3DP are its low equipment cost and its thermally-controlled sintering process. Even with reduced accuracy compared with SLM, SEBM, and LENS, Inkjet 3DP's strength of the rapid fabrication of biometallic devices at low costs makes it a suitable technique for biomedical applications [100].

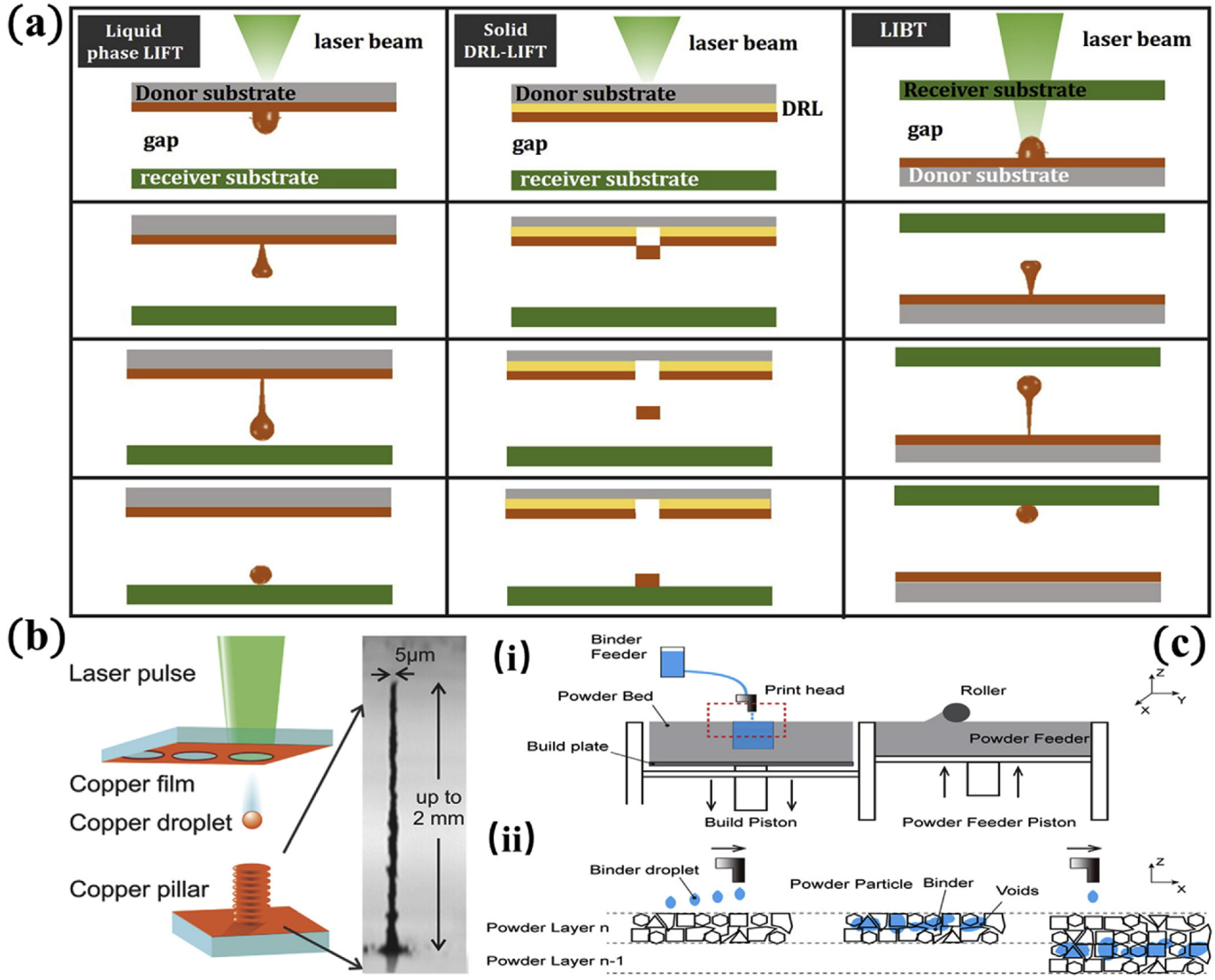

Fig. 4. (a) Schematic depiction of LIFT process [89]; (b) copper and gold pillars manufactured by LIFT with a resolution below 5 μm and height up to 2 mm [97]; (c) schematic illustrations of the 3DP process: (i) 3DP inkjet printing system, (ii) zoom-in image of marked region in i: powder/binder interaction between adjacent layers [98]. Reprint with permission. LIFT, laser-induced forward transfer.

3. 3D printing of biometals

Owing to its capability of mass production as well as customized fabrication, 3D printing technology combined with scanning and imaging technologies (CT, MRI, ultrasonic tests, etc.) provides more rapid, economical, and effective solutions for medical treatment, changing the supply chain of the existing medical industry. The scope of applications of 3D printing technology is expanding. The US Food and Drug Administration has already issued market licenses for some 3D printed medical devices. Presently, the application of 3D printed biometals in the medical device industry mainly involves five aspects and is summarized in Table 2.

In this section, the real-life applications of several biometals enabled by 3D printing technology are presented and some ongoing researches on 3D printing new biometals are discussed.

3.1. Titanium alloy

Titanium and titanium alloys, which have been used widely as biomedical implant materials since the 1970s, possess desired properties for biomedical applications, such as excellent biocompatibility, good corrosion resistance, and high ratio strength [6,7,101]. The biomedical applications of titanium alloys mainly include dental and orthopedic implants, bone screws and plates, artificial joints, artificial hearts, pacemakers, cardiac valve prostheses, and cornea backplates [102–105]. Currently, the preferred metals for biomedical applications, which are used in 90% of traditional orthopedic implants, are titanium alloy Ti6Al4V (Ti-64) and commercially pure titanium (CP–Ti).

Dense metal implants cause stress shielding effects because of their density, stiffness, and modulus of elasticity being much larger than bone tissue [58,106]. 3D printing technology can not only create personalized parts and devices but also significantly improve the process of making implants with porous microstructures. As an example, titanium alloy powder can be printed to create 3D porous metal implants. Through variations of the gradient aperture, differentiated pores, and the formed 3D penetration between pores, the elastic modulus of the metal prosthesis can be modified based on the design [76,107]. Moreover, studies have shown that porous titanium alloy implants possess good bone ingrowth ability, support the growth of human bone cells, and form a strong twist lock between the implants and bones, significantly increasing the success rate of the implants [108]. Another notable feature of porous structure is its high surface area. Surface modification

Table 2
Application fields of 3D-printed biometals in medical devices.

Application field	Objectives	Benefits
General-purpose complex implants	Provide complex-structure implants for general purposes including hip, knee, shoulder, oral implants, and so on.	Metal implants with complex 3D internal structures can be produced by 3D printing technology with high speed and high precision.
Personalized permanent implants	Solve the problem brought by the mismatch between general-purpose implants and patients with individual differences such as poor adaptability, intraoperative incomplete coverage, implant wear and loosening, and so on.	3D printed metal implants can be custom designed and fabricated into specific structure to meet the individual requirements of different patients, and thus become a personalized treatment.
Porous implant prosthesis	Circumvent the stress shielding effect brought by the dense metal implants due to the mismatch of stiffness and elastic modulus between them and human bone tissue	3D printing technology is significantly superior to traditional machining methods in constructing porous metal implants
Personalized surgical tools	Reduce the long processing cycle for traditionally personalized surgical tools	Personalized surgical tools fabricated by 3D printing technology enable more precise procedures, simplify the operation, and increase the operational speed and efficiency.
In vitro medical devices	Provide *in vitro* medical models and devices such as prosthesis, hearing aids, dental surgery template models, and so on.	With 3D printing technology, simulation models of human tissues and bones can be printed out in advance, which allows surgeons to practice the operation procedures, thus enabling more accurate and safer actual surgical operations.

(chemical grafting, deposition film, nanotopological structure, etc.) can improve the surface biological activity, wear resistance and anti-coagulation of porous medical metal implants produced by 3D printing. Biofunctional 3D printed porous surfaces of medical metal implants can further promote the stability and long-term effectiveness [109,110]. The ability to integrate with the bone bed enables bone healing at the prosthesis–bone interface, thereby prolonging the life of the prosthesis. The 3D printed titanium alloy implant can be personalized according to individual's features to more efficiently fit the patient's body. Titanium is one of the best known metal materials for biological performance. Its market demand for 3D printing in the medical field will continue to expand, and its application prospects will continue to broaden. Currently, SLM and EBM are the most commonly used techniques for 3D printing titanium alloys [58]. Clinical histology experiments have shown that 3D printed implants have a faster osseointegration rate than conventional implants [111,112].

Hollander et al. [113] studied the SLM molding process using Ti6Al4V powder, and their results showed that a titanium alloy vertebra formed by SLM has good biocompatibility and could be used to replace biological parts. In addition, the biocompatibility of titanium alloy implants manufactured via SLM or EBM has been demonstrated [81, 114–117]. For example, Palmquist et al. [118] evaluated the osseointegration of EBM-printed cylindrical and disk-shaped porous and solid Ti6Al4V implanted bilaterally in the femur and subcutaneously in the dorsum of sheep. The results exhibited that, after a 26-week implantation, both porous and solid implants were sufficiently osseointegrated, and the porous implants had a high contact rate with the bone, up to 57%. Pobloth et al. [119] fabricated two mechanically distinct titanium-mesh scaffolds with honeycomb-like structure by 3D printing through a laser sintering process and then implanted these two scaffolds into sheep tibia to investigate the effect of these implants on endogenous bone defect regeneration. The design of the scaffolds reduced stress shielding around tibial fractures and resisted mechanical failure. The results of this study indicated that mechanically optimized titanium-mesh scaffolds prepared by 3D printing can promote bone generation in large animal bone defects (Fig. 5a–i) [119]. In addition to these results from research study, several surgeries successfully implanting 3D printed titanium implants have been reported in recent years. These reports demonstrate that personalized medical implants reduce operation and hospitalization times, thereby reducing overall medical costs.

In 2011, the first clinical transplant operation was carried out with a patient-specific jaw implant fabricated by a 3D printer for an 83-year-old female patient [120]. The woman's lower jaw had chronic bone infection. Owing to her age, jaw reconstruction would have been a risky surgery, while the use of 3D printing techniques enables the development of a titanium jaw implant within a day. Both the surgical implantation time and weight of the device were shorter than that of traditional mandible implants.

The first surgery implanting a 3D printed titanium heel prosthesis was performed in 2014 on a 71-year old male patient [121], who had been facing leg amputation below the knee after being diagnosed with calcaneus cancer. The printed calcaneus heel implant was designed based on his specific defect. The implant included smooth surfaces that were in contact with his bone tissue, holes for suturing it in place, and rough surfaces that promoted enhanced tissue adhesion.

In 2015, a patient with degenerative cervical problems successfully underwent a spinal fusion with a personalized 3D printed titanium implant [122]. The printed implant possessed a precise trabecular bone prothesis featuring nanostructure that could facilitate improved healing and fusion of the patient's bones. The biomechanical properties of the implant allow it to integrate with existing bones, thereby preventing the need for re-implantation. Titanium implants made by SLM provide an ideal scaffold for the growth of bone cells and vascular structures, and when coupled with personalized designs, better results are obtained. Not only does it reduce the cost of implants, but personalization provides better-fitting medical devices, faster and easier surgery, and improved patient recovery.

In the same year, the first surgery to implant a 3D printed titanium prosthesis into the palm of the human hand was successfully performed (Fig. 6) [123]. The female patient's phalanges deteriorated because of a tumor. Traditionally, a section of bone is removed from the hip or leg of the patient and then is implanted as a thumb bone; however, these implanted phalanges are not flexible after surgery. This titanium implant was made to counteract this problem. A surgery implanted the prosthesis and connected the titanium phalanges to the nearest tendon. This success of implanting a 3D printed titanium alloy thumb is significant because it proves the viability of applying the technology to other bone replacements.

In 2017, a surgery was successfully completed to replace the entire cervical spine with a 3D printed titanium alloy artificial vertebral body. A 28-year-old female patient was diagnosed with a chondrosarcoma that eroded her second through seventh cervical vertebrae. As a result, all the vertebral bodies in the 7 cervical vertebrae were replaced with 3D printed titanium alloy prostheses. The six cervical vertebrae were surgically removed, and the new stent was reconstructed to fulfill the function of the cervical spine in supporting the head. Based on this situation, a customized artificial vertebral body that matched the patient's cervical vertebral curvature and length based on her CT and magnetic resonance images was

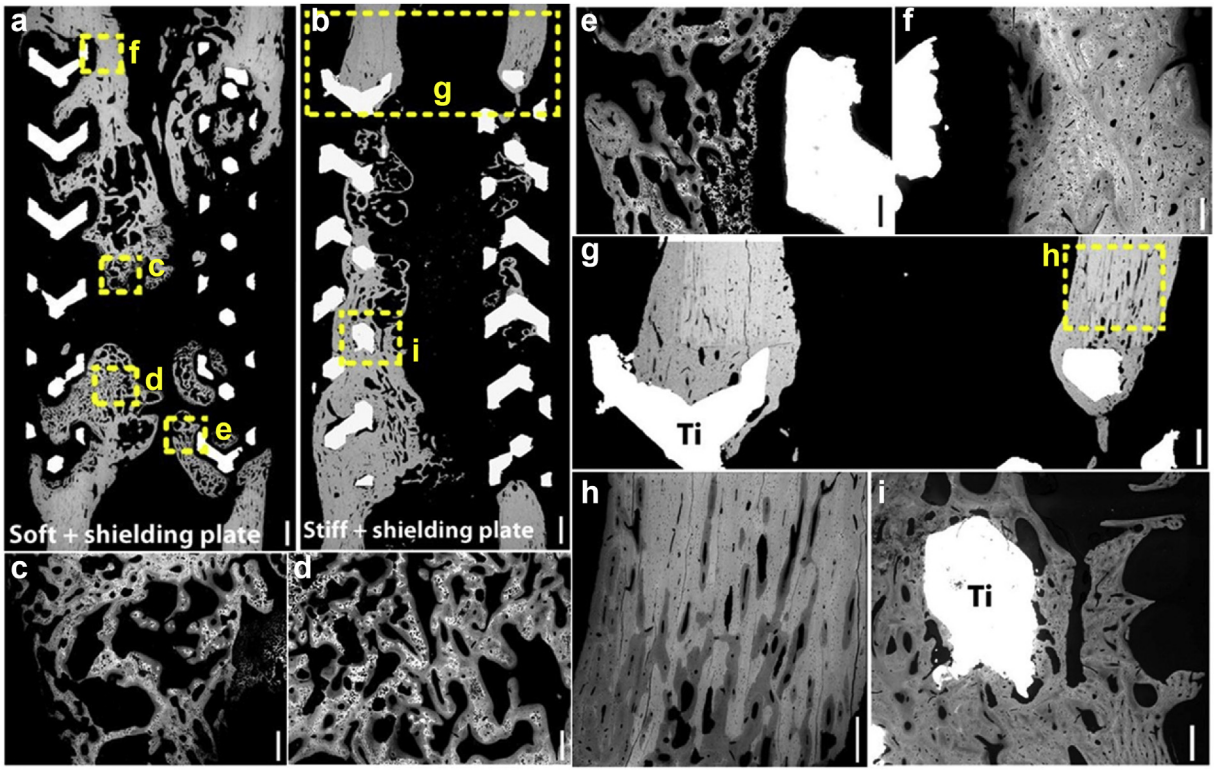

Fig. 5. Backscattered scanning electron microscopy images showing bone regeneration in the soft or stiff titanium-mesh scaffolds: (a) soft and shielding plate; (b) stiff and shield plates; (c)–(e) bone regeneration with lower mineralization and less dense organization indicated by the woven bone appearance (darker gray areas) around scaffolds; (f) older dense plexiform bone (brighter gray areas) with higher mineralization existed close to the adjacent tibia; (g) the lamellar bone (brighter gray scale), with higher mineralization than the plexiform bone, adjacent tibia; (h) bone density reduction of the cortical is appeared at the interface of adjacent scaffold; (i) bone-scaffold direct contact in the still scaffolds [119]. Reprint with permission.

developed. The 3D printed prosthesis has a sponge-like micropore structure, promoting the adjacent bones' growth into implant. Ultimately, the prosthesis and human bone became fused. The connection between the patient's head and body by the metal implants was confirmed with X-ray imaging after the operation. This successful case indicates that 3D printed titanium implant could be used for large-scale replacement surgeries.

3.2. Tantalum

Tantalum (Ta) has been used in dental and orthopedic fields as vascular clips, radiographic bone markers, and nerve repair materials, and cranial-defect repair materials since the 1940s because of its excellent biocompatibility and good chemical stability [3,10,11,124]. However, tantalum applications were once limited by the high manufacturing

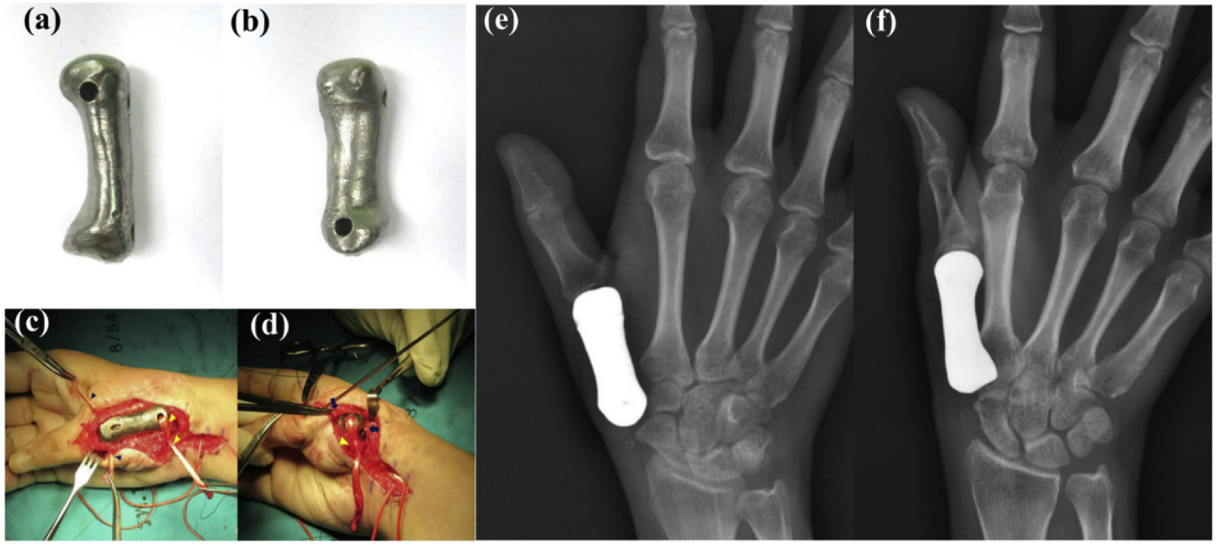

Fig. 6. (a)–(b) Photographs of anterior aspect and volar aspect of prosthesis before implantation; (c)–(d) intraoperative photographs showing 3D printed titanium first metacarpal prosthesis with the ligament reconstruction in the proximal and distal portions; (e–f) plain radiographs of a patient-matched total first metacarpal prosthesis [123]. Reprint with permission.

cost and the infeasibility of fabricating modular implants using Ta [125]. To date, porous tantalum implants have been developed for osteogenesis applications, such as bone graft substitutes. Hip, knee, and spinal prostheses made from tantalum have been used widely in surgery. A stable bone–implant interface and dense bone growth into porous tantalum in a canine model have been demonstrated by using acetabular cups and cylindrical implants [126,127]. Currently, there are several clinical reports on porous tantalum implants, including acetabular cups, tibial, and spinal implants [11,128]. These clinical studies have validated the application of porous tantalum implants in various clinical environments [11,129]. In addition, many studies have attempted to fabricate porous or solid tantalum parts using new manufacturing techniques such as LENS [130], spark plasma sintering [131], and SLM [132,133]. Balla et al. [125] coated Ta on Ti by LENS for the first time, and the Ta coating improved significantly the osseointegration properties compared with the Ti surface. Subsequently, they also used LENS to prepare Ta porous structures with varying porosity [130]. The manufacturing method allowed product's Young's modulus to range from 1.5 to 20 GPa by adjusting the porosity between 27% and 55%. Moreover, porous tantalum structures promote cell adhesion, proliferation, differentiation, and even early biofixation. Meanwhile, Thijs et al. [133] reported functional tantalum parts fabricated by SLM. SLM can produce strong parts with almost zero porosity because of its complete dissolution of tantalum powder. Wauthle et al. [132] used SLM to make pure tantalum implants with interconnected open pores. Compared with porous Ti6Al4V, the porous pure tantalum prepared by SLM exhibits excellent bone osteoconductive properties, higher normalized fatigue strength, and high ductility, It is expected that porous tantalum implants produced by SLM technique with tunable mechanical properties and predictable biological properties would be widely used in orthopedics.

In 2017, the world's first surgery to repair a severely deficient knee joint by implanting a 3D printed tantalum artificial joint cushion was accomplished into an 84-year-old male patient's body. The primary significance of this surgery is that it was the first operation to use tantalum in a clinical implant. The data of patient's knee joint's shape, density, and defects were obtained with a 3D CT scan; based on which, the personalized tantalum cushion was manufactured with 3D printing. Across a variety of patients, the shape of bone defects also varies, and the existing standardized metal pads cannot completely reconstruct defective bone structures for every patient. Currently, most 3D printed joint pads are made of titanium. Compared with titanium, tantalum has better biocompatibility and supports enhanced bone ingrowth. These make it a better candidate as base material for implants. However, one major drawback of tantalum is that its melting point exceeds 3000 °C. As a result, most of the 3D printing equipment on the market cannot work with tantalum powder. To overcome this problem, a personalized 3D printed tantalum pad was fabricated by SLM. The shape of customized pads fabricated by this process has a good fit as well as a suitable surface roughness that can fill many bone defects. Such prosthesis greatly simplified the surgical procedure by reducing the operation time and ensuring initial stability after implantation. In addition, the rough and porous metal trabecular bone on the surface of the tantalum pad quickly induced autologous bone ingrowth, thereby obtaining long-term stability of the prosthesis as well as reducing surgical complications.

3.3. Cobalt–chromium alloy

Cobalt–chromium alloys are superalloys composed primarily of cobalt and chromium. They have excellent corrosion resistance and mechanical properties. Parts made of Co–Cr alloys have high strength, excellent wear resistance, high temperature resistance, and outstanding biocompatibility, which make them ideal load-bearing implants [5,134–137]. Co–Cr alloys were first used in artificial joints and have now been commonly used in dental and oral applications [138,139]. Because they do not contain harmful elements such as nickel and antimony, 3D printed Co–Cr alloy porcelain teeth have become the first choice for non-precious metal porcelain devices [140,141]. España et al. [142] used LENS to fabricate first CoCrMo alloy samples with porous core and solid wall, which possessed 10%–18% average total porosity and modulus of 33–43 GPa. Moreover, there are extensive studies on the microstructure [141,143–147], mechanical properties [141,144,145,148,149], corrosion behavior [141,145], and biocompatibility [150] of Co–Cr alloys prepared by SLM for dental applications [140,151]. These studies have shown that 3D printed Co–Cr alloy dental implants can accurately mimic the natural structure of the alveolar bone. Their surfaces are densely covered with 3D through-grooves which induce the regeneration of osteoblasts in the cavity [141]. Hazlehurst et al. [152] managed to use SLM to fabricate cobalt-chrome-molybdenum cellular structures with volumetric porosity ranging from 25% to 95% (Fig. 7a). The stiffness and strength of these cellular structures are similar to those of cortical bone and cancellous bone in the human femur. It has been demonstrated that porous structure could reduce the effective modulus of implants by 75–80% and minimize stress shielding, matching the implant properties with bone tissue and enhancing long-term osteointegration stability [153]. Demir et al. [154] explored the fabrication of Co–Cr alloy cardiovascular stents (Fig. 7b and c) using different scanning processes of industrial SLM systems. It is found that the single-step process of SLM can replace both the extrusion and tube drawing production and continuous laser microdissection required by the conventional techniques. Direct mesh shape manufacturing cannot be performed by these methods because of the required surface quality and mechanical properties. SLM 3D printing technology can combine microtube fabrication and laser microcutting processes into a single step, which further reduces fabrication time. It is reasonable to expect that in the near future, SLM would surpass the traditional stent manufacturing methods to become the primary selection of the industry.

However, as load-bearing implants, CoCr alloys still have wear and corrosion problems when they are placed inside human body, leading to material loss of the implant. The resulting release of metal ions will lead to various medical complications. Sahasrabudhe et al. [155] showed that the addition of calcium monophosphide (CaP) into CoCrMo alloys could decrease the wear rate. They prepared CoCrMo alloys with 3% CaP by LENS 3D printing and the sample wear rate was only one third compared to that of pure CoCrMo alloys. The release of Co^{2+} and Cr^{2+} also reduced to four times less than that of pure CoCrMo alloy without CaP.

3.4. Magnesium

Internal fixation implants used in global orthopedic clinical operations mainly include titanium alloys and stainless steels. Implants made from both materials are not degradable in the human body and require a second step to adjust or remove them. Moreover, the use of inert biometals would cause long-term complications. Owing to these problems, implants made of degradable biometals are required [14]. As a result, magnesium alloys draw people's attention. When they are used in implants, a second-step operation is often unnecessary [157,158]. Magnesium alloys have the best biomechanical compatibility with human bone (because its similar density) and have minimal associated discomfort compared to stainless steel or titanium alloys [14,158,159]. Furthermore, magnesium can be absorbed by the human body and the released as magnesium ions to enhance the proliferation and differentiation of osteoblasts, thereby accelerating bone growth and healing [160–162]. In addition to medical equipment such as bone screws and bone plates, magnesium alloys can also be made into degradable cardiovascular stents [163,164]. Although magnesium alloys are considered as one of the most challenging materials to process via laser powder bed fusion because of their flammability, the demand for additive manufactured parts composed of magnesium alloys is growing. So far, there have been several studies conducted to study the influences of SLM process parameters and Mg powder properties on the densification, processing [65,165–167], and microstructural and metallurgical defects of 3D printed Mg parts by SLM [65,165,168–170].

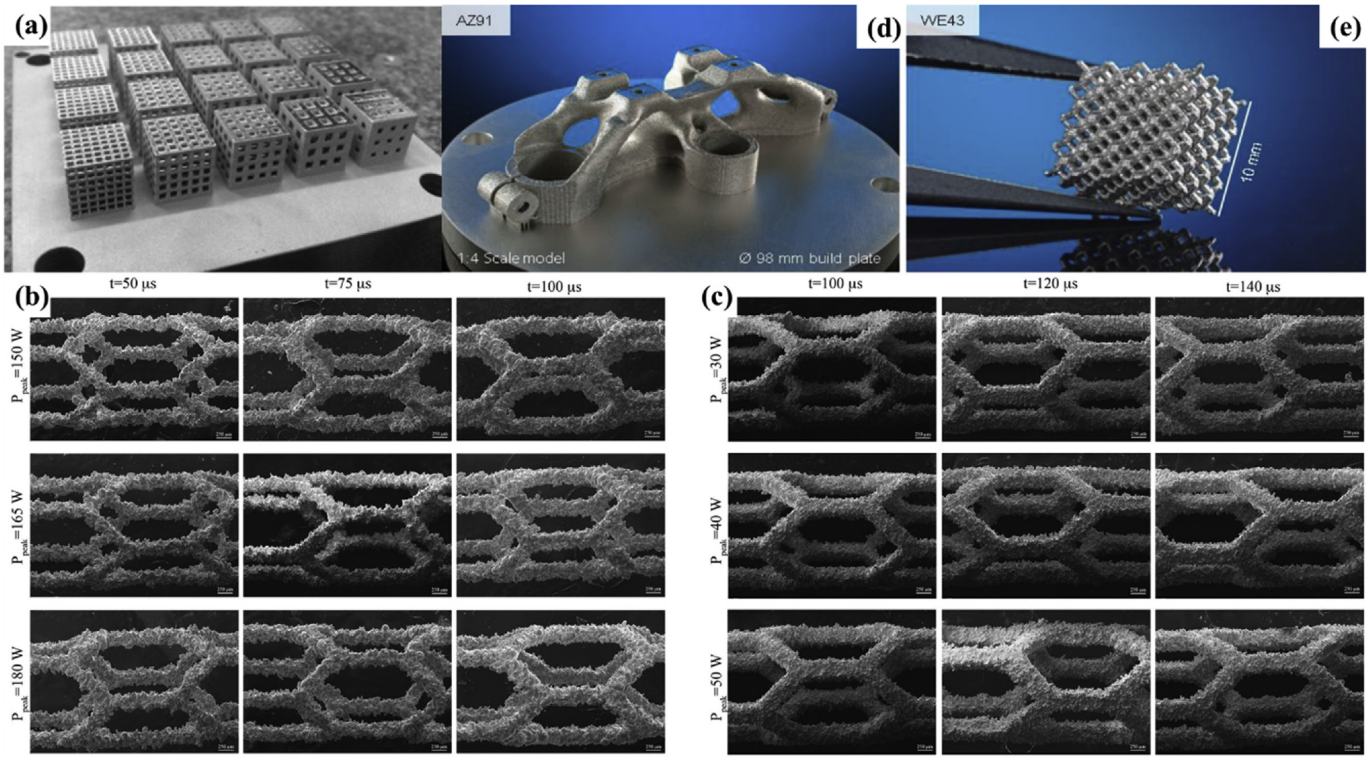

Fig. 7. (a) Square porous CoCrMo cellular structures with varying porosities created by SLM [152]; SEM images of the CoCr stents prepared by the SLM with different process parameters; (b) hatching and (c) concentric scanning strategies [154]; reprint with permission. (d)–(e) Technology demonstrations made of magnesium alloys printed by SLM: (d) a topological optimized triple clamp with a 1:4 scale model; (e) a biodegradable scaffold with designed interconnected porosity [156] (© European Powder Metallurgy Association (EPMA). First published in the World PM2016 Congress Proceedings).

3D printing techniques have been demonstrated to be able to produce complex structures made from most conventional biometals, but for magnesium and other biodegradable metals, this technology has not been widely used. Recent research showed that AZ91D magnesium alloy can be processed with wire and arc additive manufacturing [171]. Jauer et al. [156] successfully fabricated scaffold-like structures of WE43 with interconnected porosity by means of SLM (Fig. 7d and e). Li et al. [172] reported a topographically ordered and fully interconnected porous biodegradable WE43 scaffold fabricated by SLM, which only lost approximately 20% of its volume after 4 weeks and still maintained mechanical properties required for trabecular bone support. These SLM-processed WE43 scaffolds are expected to meet all functional requirements of the ideal bone substitute.

In addition, Li et al. [173] used low-temperature 3D printing technology to prepare a magnesium-containing degradable polymer for bone repair. Magnesium with osteogenic and angiogenic activity was uniformly incorporated into a PLGA/TCP (glycolide-lactide copolymer/tricalcium phosphate) degradable porous scaffold. The physical structure of PLGA/TCP/Mg as well as the orderly distribution and concentration of tricalcium phosphate and magnesium metal can be controlled by 3D printing. The designed microstructure gives this product an ideal bone-producing structure with highly interconnected pores that enhance bone cell adhesion, proliferation, migration, and tissue growth. Meanwhile, the macroscale structures can be designed to match the shape and size of the damaged area in patients'. bodies to achieve personalized repair. This magnesium-containing degradable polymer bone repair material exhibits good biocompatibility and biological activity, possesses mechanical strength matched with that of cancellous bone, and significantly improves the regeneration and angiogenesis of the implant. The inkjet 3D printing technique was used to fabricate the matrix of struvite ($MgNH_4PO_4$. $6H_2O$) and newberyite ($MgHPO_4$. $3H_2O$) through a hydraulic setting reaction between $Mg_3(PO_4)_2$ powder and binder liquid including 2 M K_2HPO_4, 0.5 M $(NH_4)_2HPO_4$, or 20% H_3PO_4. The compressive strength increased up to 10 MPa for the posthardening 3D printed struvite and increased up to 36 MPa for the posthardening newberyite, which shows a rise in range of 1.3–2.8 MPa. With its good qualities, this magnesium phosphate matrix prepared by 3D printing technique is expected to serve as a biodegradable bone substitute [174].

3.5. Iron

Iron is one of the essential trace elements in the human body and participates in various physiological reactions. Currently, iron-based materials are considered as a promising candidate for making biodegradable implants because of their excellent mechanical properties and degradability. Results of preliminary in vivo experiments have demonstrated that no local or systemic toxicity was caused by pure iron stents implanted into porcine aorta [15,175–178]. This is because of that iron ions released after degradation can be absorbed by the body to be metabolized without accumulation. However, the degradation rate of pure iron in physiological media is lower than the required degradation rate in body [15,175,176,179]. To date, a series of Fe–Mn alloys have been developed to accelerate the degradation rate of iron-based materials [175,179]. Iron-based degradable metals were among the first metals as 3D printed scaffolds used in biomedical applications [180]. 3D printed Fe–30Mn biodegradable scaffolds with a porosity of 36.3% (Fig. 8a–d) [181], fabricated by an inkjet 3D printing technique, were explored as a material for craniofacial applications. This 3D printed scaffolds formed a mixed phase alloy of martensite ε and austenite γ phase after subsequent sintering. Its corrosion rate was much faster than that of pure iron, and the corrosion product contained calcium and phosphorus. As a result, its tensile mechanical properties were like those of natural bone, thus reducing the risk of stress. Besides this, the Fe–30Mn scaffolds also demonstrated excellent cytocompatibility. In addition, Chou et al. [181] systematically studied the effect of the composition of the Fe–Mn alloy on the degradation rate using the CALPHAD (calculation of phase diagram) theoretical model. With Ca

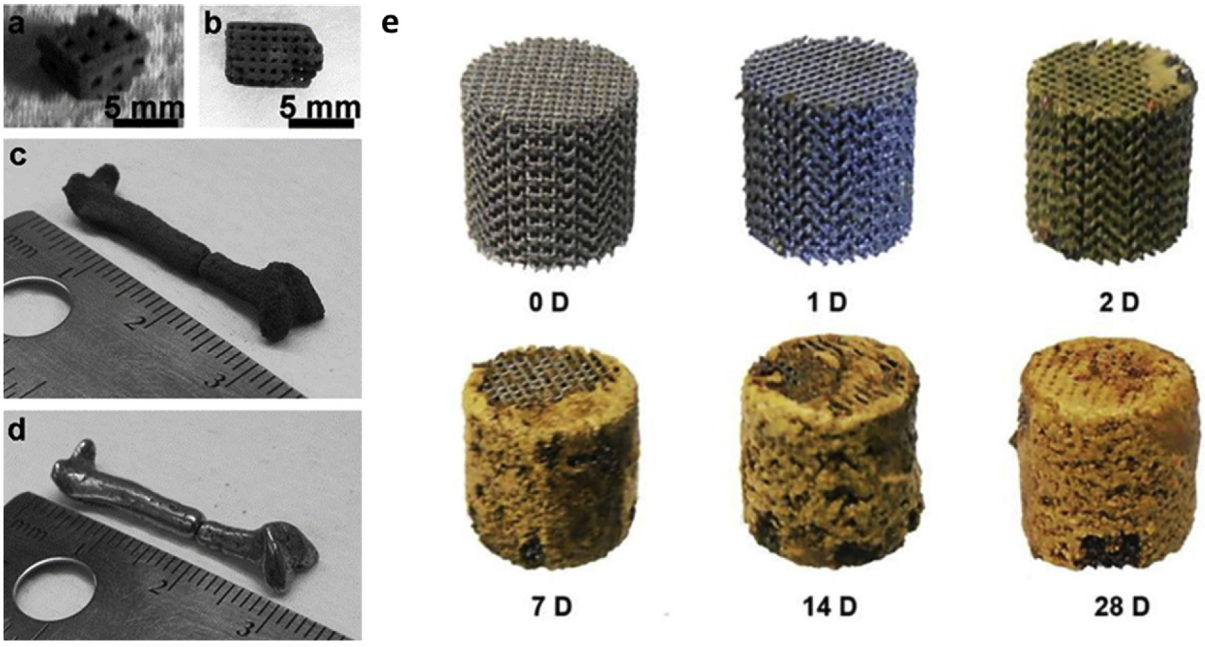

Fig. 8. Photographs of 3D printed prototype parts with different square pore sizes made of Fe–30Mn powder after sintering: (a) 1-mm length, (b) 500-μm length. Before humble-finished (c) and after tumble-finished (d) miniature human femur [181]; (e) visual inspection *in vitro* degradation behavior of as-degraded iron scaffolds [183]. Reprint with permission.

and Mg elements introduced, the study shows Fe–Mn, Fe–Mn–Ca, and Fe–Mn–Mg alloys all exhibited cytocompatibility. Among them, Fe-35 wt % Mn alloy showed improved degradation rate compared with Fe–30Mn. Fe–Mn and Fe–Mn–1Ca were then printed by binder-jet 3D printing to form solid 3D constructs. Both exhibited excellent cell compatibility [182]. Li et al. [183] first reported the preparation of topologically ordered porous iron scaffolds (Fig. 8e) using direct metal printing (DMP) and studied the effect of the DMP process on the surface area and grain size of the scaffolds. The results showed that even after 4 weeks of degradation, the mechanical properties of the porous scaffold were still within the tolerable limits of trabecular bone, and the degradation rate was 12 times faster than that of the cold-rolled iron with only 3.1% weight loss. This porous iron scaffold also exhibited cytocompatibility.

Beyond iron-based alloys, there are many investigations focused on iron and iron oxide particles. Zhang et al. [184] used a 3D Bioplotter to print composite scaffolds containing magnetic Fe_3O_4 nanoparticles and bioactive glass/polycaprolactone (Fe_3O_4/MBG/PCL). These composite scaffolds had uniformly distributed 60% porosity of size 400 μm, and a compression strength of 13–16 MPa. The addition of magnetic Fe_3O_4 nanoparticles gave the scaffold a magneto-thermal effect which significantly promotes the cellular biological properties. In addition, doxorubicin anticancer drugs were loaded into this scaffold to enhance the osteogenic activity while achieving sustained drug delivery. Liu et al. [185] used polydimethylsiloxane doped with iron particles to fabricate artificial magnetic cilium by 3D extrusion printing. In summary, 3D printed biodegradable porous scaffolds made of iron-based alloys are able to promote bone regeneration without complications and therefore become good candidates for orthopedic implants. It is predictable that in the future, 3D printing–enabled degradable iron-based medical devices would be superior to implants produced by conventional techniques as 3D printing could accurately print implants with complex structures and dimensions that meet specific bone defect requirements of patients and thus facilitate personalized treatment.

3.6. Zinc

Zinc (Zn) is one of the indispensable trace elements in the human body. It is directly involved in enzyme synthesis, nucleic acid metabolism, gene expression, signal transduction, apoptosis regulation, growth promotion and tissue regeneration in the body [186]. In 1996, Hennig et al [187] discovered that Zn also exhibited strong anti-atherogenic properties. Although there are still concerns about whether the utilization of Zn metal in the human body can cause undesirable consequences, studies have shown that the toxicity of zinc is negligible. Zn has also been proven to have antibacterial activity [188]. Recently, zinc has gradually replaced iron and magnesium alloys to be used to fabricate degradable medical implants because it has an almost-ideal degradation rate between that of iron and magnesium. This property makes it and its alloys promising candidates to serve as degradable cardiovascular stents and dental implants [14,16,189,190]. There have been some studies conducted on the design [191,192], fabrication [14,193], and degradation mechanisms *in vitro* [193–195] and in vivo [190, 196–199] of zinc alloys. Although biodegradable Zn implants with patient-specific customization can be processed by SLM, the low melting point, high oxidation tendency, and low boiling point of Zn usually result in high porosity in the fabricated parts. Recently, reports have been published on the preparation of 3D printed Zn metal using SLM. Demir et al. [200] first studied the fabrication of biodegradable pure Zn implants using SLM, and proposed the parameters for fabrication process. The oxidation level of the 3D printed zinc parts was equivalent to that of the pure zinc powder (approximately 2 wt%). The microhardness of the 3D printed zinc parts was 42 HV, which was slightly higher than the pure Zn counterpart because of the high cooling rate in the SLM process. SLM can adjust the density, microstructure, and geometry of 3D printed Zn parts, which determine the mechanical properties and degradation of Zn products. Wen et al. [201] studied the influences of SLM process parameters on the surface quality, densification, and mechanical properties of pure Zn components. Solid pure zinc parts with fine columnar grains and density over 99.50% can be prepared by SLM. The surface roughness after sandblasting decreased to 4.83 μm from 9.15 to 10.79 μm in the as-melted status; the roughness is equivalent to the optimal results of SLM-prepared common metals. These mechanical strengths, such as elastic modulus (23 GPa), yield strength (114 MPa), ultimate strength (134 MPa), hardness (42 HV), and elongation (10.1%), were superior to those of the components produced by conventional manufacturing methods. Pure Zn cardiovascular stents (Fig. 9a–c) [201], with stent

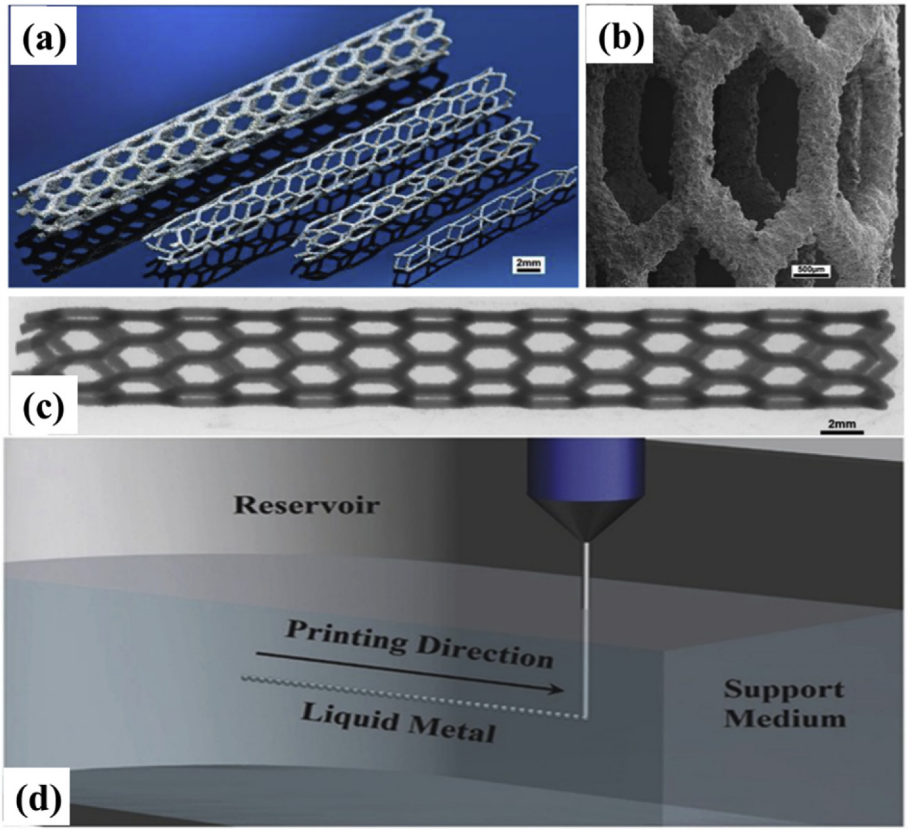

Fig. 9. SLM-fabricated zinc cardiovascular stents: (a) optical photograph, (b) SEM images of the struts, and (c) X-ray graph of stent by CT machine [201]; (d) a schematic of the suspension 3D printing method for liquid metal [202]. Reprint with permission. SLM, selective laser melting; CT, computed tomography; SEM, scanning electron microscope.

diameter of 2–5 mm and strut diameter of 200–500 μm, were also 3D printed by SLM. The results of the current studies suggest that SLM will replace traditional processing methods for solid pure Zn parts and topographically ordered pure Zn cardiovascular stents, which have an encouraging prospect in the biomedical field.

3.7. Liquid metals

Liquid metal is a type of functional material with very unique physical and chemical behaviors. This family includes mercury (Hg, −39 °C), gallium (Ga, 30 °C), gallium alloys (<30 °C), francium (Fr, 27 °C), cesium (Cs, 29 °C), and rubidium (Rb, 40 °C) [203]. Mercury is the most common liquid metal, but its applications have been limited because of its toxicity. Gallium-based alloys, for example, gallium-indium-tin (Galinstan) and eutectic gallium-indium (EGaIn), are promising alternatives to Hg as they have low toxicity [203]. Recently, the value of liquid metals in biomedicine has become more apparent. Liquid metal has been utilized to solve a series of major biomedical problems, bringing conceptual revolutions to medical technology. For example, liquid metal has been used for nerve connection and repair. Furthermore, it has been used for angiography, embolization for vascular tumor treatment, alkali metal fluid thermochemical ablation for tumor treatment, injectable solid-liquid conversion for low-melting metal cement, flexible exoskeletons, printed flexible radiation protection, injectable implantable medical electronics, and direct-printed electronic circuits on human skin. Its use in a diverse set of applications has gathered widespread attention as technological breakthroughs continue [204,205]. Liu et al. [206] facilitated signal transduction by suturing a silicone tube encapsulating liquid gallium to both ends of a damaged sciatic nerve in mice. Electrophysiological tests showed that muscle atrophy was delayed by two months in mice after liquid metal surgery compared with the control group. This work further validated the potential of liquid metals in the field of nerve repair. Furthermore, Li et al. [207] also confirmed that the low-voltage electrical effects based on liquid metal's conduction on the skin can effectively treat malignant melanoma. The authors additionally explored the printing and packaging features, washable properties, and constraints of liquid metals on different fabrics. They demonstrated that the liquid metal can be used in a flexible infrared monitoring module controlled by a mobile phone, which indicated that liquid metals are expected to play a key role in wearable medical devices in the future [208].

In terms of 3D printed liquid metals, Yu, et al. [202] was able to perform suspension 3D printing for liquid metal (Fig. 9d) using a hydrogel as a transparent support medium. These hydrogels had mechanical properties between those of a solid and a liquid as well as self-healing capabilities. The printing method overcame the technical challenges caused by high surface tension, low viscosity, easy flow, and heavy weight of the liquid metal ink. During the manufacturing process, the hydrogel could be freely and rapidly converted between solid and liquid states, so it can exert a viscous force to liquid metal droplets. The metal droplets extruded by the nozzle were first separated from the nozzle by the relative movement between the nozzle and hydrogel; then, the droplets were wrapped and fixed in the support hydrogel. The desired 3D structure was able to be formed through the layer-by-layer stacking of metal microspheres along the printing path. The printing accuracy can be regulated by the needle size, printing speed, and the gel environment. Both the liquid metal and hydrogel are flexible materials; therefore, the constructed stereoscopic electronic devices are stretchable and can be deformed. This research has important value in the fields of amorphous flexible electronic devices, rapid manufacturing of intelligent systems, and deformable 4D printing. Moreover, Jin et al. [28] demonstrated an alternative method for directly preparing 3D medical electronic devices in vivo by sequentially injecting liquid metal ink and biocompatible

packaging material. Various medical electrodes can be easily formed at target locations and printed to fit the structure of target tissues. In vitro results demonstrated excellent performance of these injection electrodes, and in vivo results revealed that the prepared electrodes could be used simultaneously as high efficiency electrocardiogram electrodes and stimulating electrodes. These studies shed light on the unique characteristics of injectable liquid metal–based 3D medical electronics, opening the door to direct in situ fabrication of electrophysiological sensors and therapeutic devices.

4. Future direction and challenges

Nowadays, 3D printing has become a key technology in the medical field because of its ability to customize implants according to each individual's needs. At present, as the world's population of elderly people is rapidly increasing, the demand for personalized medicine and customized 3D printed medical devices, especially surgical implants and orthopedic instruments, is very intensive. Therefore, 3D printing–enabled metallic implants are now playing a crucial role in the medical device market. 3D printing technology brings many incomparable advantages, including the capability of having personalized designs, the fabrication of structures with complex geometries, and the reduction of manufacturing time and medical costs, in the preparation of metallic medical devices. However, this method is still in its infant stages for biomedical applications, and there are many challenges before its clinical use is widespread.

First of all, 3D printing techniques for metallic materials are not as well established as those for conventional manufacturing methods. At present, even for the most utilized EBM technique, there is still a lot of room for improvement. The interaction between the electron beam and metal powders, the control of residual stress, the surface roughness, the internal structural defects, and other key technical problems and stability issues all need to be optimized. The accuracy and efficiency of the 3D printing production of metals are currently not sufficient. Factors such as the material properties and processing and equipment capabilities make it difficult to directly manufacture parts with high precision and good surface finish, while simultaneously achieving high manufacturing efficiency, as there is always a trade-off between the printing accuracy and speed. Moreover, as most 3D printing techniques adopt a layer-by-layer printing process, even if the bonding between each layer is very tight, there are still many defects in the product's rigidity and strength, leading to poor performance of the finished products. Figuring out how to achieve the high accuracy (even at microprocessing/nanoprocessing scales), excellent surface finish, strong physical and mechanical product properties, and fast-speed manufacturing is an urgent problem must be solved before 3D printing technology can be applied on a large scale for the medical device field.

In addition, more high-quality raw materials are needed for printing. Current raw materials for 3D printing, owing to different molding principles, are generally powdery or filamentous, which need to meet more specific requirements than common solid materials. For example, there are stricter quality requirements for the size, size distribution, uniformity, oxygen content, and fluidity. Furthermore, these materials need also to meet biological requirements for medical device applications to prevent various biological risks. However, there are only a few well-established materials available for 3D metal printing such as titanium alloys, stainless steel, and aluminum alloys. Compared with traditional 3D printing, this number is very small, and currently, the lack of raw materials remains the most important limiting factor metal 3D printing technology faces.

Furthermore, there are issues in the current R & D of 3D printing equipment for metal fabrication. Expensive equipment procurement, maintenance costs, and consumables costs alongside printing software incompatibility severely limit the popularity and development of 3D printing technology. Today, the development trends of this technology center around improving the ‘high resolution, high throughput, high capacity’ of the device to achieve miniaturization and reduce costs as well as making the device software and hardware more compatible to assist with future upgrades and expansion.

The lack of standardization of the biosafety of 3D printed metallic medical devices is another urgent issue that needs be solved. There are extremely stringent requirements for the materials used in clinic. It is necessary to consider the safety, biocompatibility, degradation performance, and biological activity of the materials before and after printing to meet the requirements for industrialization and clinical use. For example, for medical plants made of titanium alloys, the printing processes and product performance should be evaluated before and after printing to ensure that there is no teratogenic carcinogenesis after implantation. An international standard evaluation system for such issues, however, has not been established, and there are still some pending ethical issues. Presently, more pursuits are focusing on the application of 3D printed implants in the clinical field, but a systematic understanding of the potential risks of these implants is lacking. It is necessary to keep track of the long-term outcomes of the implantation of 3D printed metallic devices and establish an evaluation system to help enhance the safety and effectiveness of these personalized medical devices.

In addition, strict sterilization of implants is one of the key parts to ensure the success of implants. Improper sterilization process has a negative impact on the surface properties of orthopedic implants and joint prostheses, leading to implant failure. Therefore, it is essential to select appropriate sterilization methods for different metal implants. With the increasing variety of 3D printed medical biometals, it is also an urgent need to find suitable sterilization methods and establish the standards for implants made of different biometals, especially for those with complex porous structure.

From the technical point, the capability of multiple additive manufacturing to simultaneously print both soft and hard biomaterials is worth more study and investigation to further extend its applications in biomedical field. Currently in many areas, especially tissue engineering, the integration of soft and hard biomaterials at the interface is crucial for the improvement of clinical outcome. It would be very significant if this kind of interface integration can be accomplished by 3D printing technology, which would reduce the cost and enhance the efficiency of the manufacturing process.

Although the application of 3D printed metals in the medical fields faces the aforementioned constraints, biological 3D printing will provide an unprecedented opportunity through the continuous development and improvement of the biomedical materials industry and 3D printing technology. We also need to recognize that 3D printed metallic implants still have a long way to go. Most of the current trials are in the research stage, and thus, wide clinical applications and large-scale production are far from realization. It is reasonable, however, to believe that 3D printing technology will play a bigger role in the metallic biomedical device field and eventually become a main part of the digital manufacturing and digital economy of medical devices that is being integrated with artificial intelligence, big data, and the Internet.

Declaration of interest

The authors declare that they have no known competing financial interests or personal relationships that could have appeared to influence the work reported in this paper.

Acknowledgments

The authors acknowledge funding from the National Natural Science Foundation of China (No. 51401126, 81401819), programs supported by Ningbo Natural Science Foundation (2018A610203), the National Institutes of Health (1R01EB021857-02, 1R01AR073135-01A1, 1R01 1 AR074234-01A1), UCLA BioEng 57179, and BiofabUSA Quick Start Project.

References

[1] N. Ashammakhi, S. Ahadian, M.A. Darabi, M. El Tahchi, J. Lee, K. Suthiwanich, A. Sheikhi, M.R. Dokmeci, R. Oklu, A.J. Khademhosseini, Minimally invasive and regenerative therapeutics, Adv. Mater. 31 (1) (2019) 1804041.

[2] M. Niinomi, Recent metallic materials for biomedical applications, Metall. Mater. Trans. 33 (3) (2002) 477.
[3] M. Niinomi, M. Nakai, J.J. Hieda, Development of new metallic alloys for biomedical applications, Acta Biomater. 8 (11) (2012) 3888–3903.
[4] C.-C. Shih, C.-M. Shih, Y.-Y. Su, L.H.J. Su, M.-S. Chang, S.-J.J. Lin, Effect of surface oxide properties on corrosion resistance of 316L stainless steel for biomedical applications, Corros. Sci. 46 (2) (2004) 427–441.
[5] J.A. Disegi, R.L. Kennedy, R. Pilliar, in: Cobalt-base Alloys for Biomedical Applications, ASTM Danvers, 1999.
[6] M.J. Niinomi, Mechanical biocompatibilities of titanium alloys for biomedical applications, J. Mech. Behav. Biomed. Mater. 1 (1) (2008) 30–42.
[7] C. Elias, J. Lima, R. Valiev, M. Meyers, Biomedical applications of titanium and its alloys, Jom 60 (3) (2008) 46–49.
[8] T. Yoneyama, S. Miyazaki, Shape Memory Alloys for Biomedical Applications, Elsevier, 2008.
[9] C. Barras, K.J. Myers, Nitinol–its use in vascular surgery and other applications, Eur. J. Vasc. Endovasc. Surg. 19 (6) (2000) 564–569.
[10] J.J. Black, Biologic performance of tantalum, Clin. Mater. 16 (3) (1994) 167–173.
[11] B.R. Levine, S. Sporer, R.A. Poggie, C.J. Della Valle, J.J. Jacobs, Experimental and clinical performance of porous tantalum in orthopedic surgery, JB (J. Biochem.) 27 (27) (2006) 4671–4681.
[12] B. O'Brien, J. Stinson, W.J. Carroll, Development of a new niobium-based alloy for vascular stent applications, J. Mech. Behav. Biomed. Mater. 1 (4) (2008) 303–312.
[13] B.J. O'Brien, J.S. Stinson, D.A. Boismier, W.M. Carroll, Characterization of an NbTaWZr alloy designed for magnetic resonance angiography compatible stents, JB (J. Biochem.) 29 (34) (2008) 4540–4545.
[14] Y. Zheng, X. Gu, F.J.M.S. Witte, E.R. Reports, Biodegradable Metal 77 (2014) 1–34.
[15] H. Hermawan, D. Dubé, D.J. Mantovani, Developments in metallic biodegradable stents, Acta Biomater. 6 (5) (2010) 1693–1697.
[16] P.K. Bowen, E.R. Shearier, S. Zhao, R.J. Guillory, F. Zhao, J. Goldman, J.W.J. Drelich, Biodegradable metals for cardiovascular stents: from clinical concerns to recent Zn-Alloys, Adv. Healthc. Mater. 5 (10) (2016) 1121–1140.
[17] I. Hwang, Z. Guan, X.J. Li, Fabrication of zinc–tungsten carbide nanocomposite using cold compaction followed by melting, JOM (J. Occup. Med.) Sci.Eng. 140 (8) (2018), 084503.
[18] I. Hwang, Z. Guan, X.J. Li, Scalable manufacturing of zinc-tungsten carbide nanocomposites, P & M (Philos. Med.) 26 (2018) 140–145.
[19] Y. Xin, T. Hu, P.J. Chu, In vitro studies of biomedical magnesium alloys in a simulated physiological environment: a review, Acta Biomater. 7 (4) (2011) 1452–1459.
[20] X.-N. Gu, Y.-F.J. Zheng, A review on magnesium alloys as biodegradable materials, Front. Mater. Sci. China 4 (2) (2010) 111–115.
[21] Z. Guan, I. Hwang, S. Pan, X.J. Li, Nano-manufacturing, scalable manufacturing of AgCu40 (wt%)–WC nanocomposite Microwires, JOM (J. Occup. Med.) 6 (3) (2018), 031008.
[22] K.V. Wong, A.J.I.M.E. Hernandez, A Review of Additive Manufacturing, 2012, 2012.
[23] I. Campbell, D. Bourell, I.J. Gibson, Additive manufacturing: rapid prototyping comes of age, Rapid Prototyp. J. 18 (4) (2012) 255–258.
[24] S. Bose, D. Ke, H. Sahasrabudhe, A.J. Bandyopadhyay, Additive manufacturing of biomaterials, Prog. Mater. Sci. 93 (2018) 45–111.
[25] B.C. Gross, J.L. Erkal, S.Y. Lockwood, C. Chen, D.M. Spence, Evaluation of 3D Printing and its Potential Impact on Biotechnology and the Chemical Sciences, ACS Publications, 2014.
[26] Y. He, Y. Wu, J.z. Fu, Q. Gao, J. Qiu, Developments of 3D printing microfluidics and applications in chemistry and biology: a review, Electroanalysis 28 (8) (2016) 1658–1678.
[27] S. Waheed, J.M. Cabot, N.P. Macdonald, T. Lewis, R.M. Guijt, B. Paull, M.C.J. Breadmore, 3D printed microfluidic devices: enablers and barriers, Lab Chip 16 (11) (2016) 1993–2013.
[28] C. Jin, J. Zhang, X. Li, X. Yang, J. Li, J.J. Liu, Injectable 3-D fabrication of medical electronics at the target biological tissues, Sci. Rep. 3 (2013) 3442.
[29] G. Ryan, A. Pandit, D.P. Apatsidis, Fabrication methods of porous metals for use in orthopaedic applications, JB (J. Biochem.) 27 (13) (2006) 2651–2670.
[30] S. Bose, M. Roy, A.J. Bandyopadhyay, Recent advances in bone tissue engineering scaffolds, Trends Biotechnol. 30 (10) (2012) 546–554.
[31] A. Jardini, M. Larosa, M. Macedo, L. Bernardes, C. Lambert, C. Zavaglia, R. Maciel Filho, D. Calderoni, E. Ghizoni, P.J. Kharmandayan, Improvement in cranioplasty: advanced prosthesis biomanufacturing, Procedia CIRP 49 (2016) 203–208.
[32] D.M. Almog, E. Torrado, S.W.J. Meitner, Fabrication of imaging and surgical guides for dental implants, J. Prosthet. Dent 85 (5) (2001) 504–508.
[33] D. Liu, J. Fu, H. Fan, D. Li, E. Dong, X. Xiao, L. Wang, Z.J. Guo, Application of 3D-printed PEEK scapula prosthesis in the treatment of scapular benign fibrous histiocytoma: a case report, J. Bone. Oncol. 12 (2018) 78–82.
[34] M.Z. Ibrahim, A.A. Sarhan, F. Yusuf, M.J. Hamdi, Compounds, Biomedical materials and techniques to improve the tribological, mechanical and biomedical properties of orthopedic implants–A review article, J. Alloy. Comp. 714 (2017) 636–667.
[35] M. Tischler, C. Patch, A.S.J. Bidra, Rehabilitation of edentulous jaws with zirconia complete-arch fixed implant-supported prostheses: an up to 4-year retrospective clinical study, J. Prosthet. Dent. 120 (2) (2018) 204–209.
[36] T. Matsushita, S. Fujibayashi, T. Kokubo, Titanium foam for bone tissue engineering, in: Metallic Foam Bone, Elsevier, 2017, pp. 111–130.
[37] V. Saikko, T. Ahlroos, H. Revitzer, O. Ryti, P.J. Kuosmanen, The effect of acetabular cup position on wear of a large-diameter metal-on-metal prosthesis studied with a hip joint simulator, Tribol. Int. 60 (2013) 70–76.
[38] U. Hedlundh, L.J. Karlsson, Combining a hip arthroplasty stem with trochanteric reattachment bolt and a polyaxial locking plate in the treatment of a periprosthetic fracture below a well-integrated implant, Arthroplast. Today 2 (4) (2016) 141–145.
[39] S.A. Tofail, E.P. Koumoulos, A. Bandyopadhyay, S. Bose, L. O'Donoghue, C.J. Charitidis, Additive manufacturing: scientific and technological challenges, market uptake and opportunities, Mater. Today. 21 (1) (2018) 22–37.
[40] W.J. Sames, F. List, S. Pannala, R.R. Dehoff, S.S.J. Babu, The metallurgy and processing science of metal additive manufacturing, Int. Mater. Rev., 61 (5) (2016) 315–360.
[41] P.K. Gokuldoss, S. Kolla, J.J.M. Eckert, Additive manufacturing processes: selective laser melting, electron beam melting and binder jetting—selection guidelines, Materials 10 (6) (2017) 672.
[42] C.K. Chua, K.F. Leong, 3D Printing and Additive Manufacturing: Principles and Applications (With Companion Media Pack) of Rapid Prototyping, fourth ed., World Scientific Publishing Company, 2014.
[43] K. Shah, Laser Direct Metal Deposition of Dissimilar and Functionally Graded Alloys, The University of Manchester, United Kingdom), 2011.
[44] L.G. Zhang, J.P. Fisher, K. Leong, 3D Bioprinting and Nanotechnology in Tissue Engineering and Regenerative Medicine, academic press, 2015.
[45] O.O. Spencer, O.T. Yusuf, T.C.J. Tofade, additive manufacturing technology development: a trajectory towards Industrial Revolution, Am. J. Mech. Ind. Eng. 3 (5) (2018) 80–90.
[46] A. Bandyopadhyay, S. Bose, S. Das, 3D printing of biomaterials, MRS Bullet. 40 (2) (2015) 108–115.
[47] J.J. Beaman, C.R. Deckard, Selective Laser Sintering with Assisted Powder Handling, Google Patents, 1990.
[48] J.-P. Kruth, P. Mercelis, J. Van Vaerenbergh, L. Froyen, M.J. Rombouts, Binding mechanisms in selective laser sintering and selective laser melting, Rapid Prototyp. J. 11 (1) (2005) 26–36.
[49] J.-P. Kruth, X. Wang, T. Laoui, L.J. Froyen, Lasers and materials in selective laser sintering, Assemb. Autom. 23 (4) (2003) 357–371.
[50] W.E. Frazier, Metal additive manufacturing: a review, J. Mater. Eng. Perform. 23 (6) (2014) 1917–1928.
[51] M. Agarwala, D. Bourell, J. Beaman, H. Marcus, J.J. Barlow, Direct selective laser sintering of metals, Read. Psychol. J. 1 (1) (1995) 26–36.
[52] D.K. Pattanayak, A. Fukuda, T. Matsushita, M. Takemoto, S. Fujibayashi, K. Sasaki, N. Nishida, T. Nakamura, T.J. Kokubo, Bioactive Ti metal analogous to human cancellous bone: fabrication by selective laser melting and chemical treatments, Acta Biomater. 7 (3) (2011) 1398–1406.
[53] C.Y. Yap, C.K. Chua, Z.L. Dong, Z.H. Liu, D.Q. Zhang, L.E. Loh, S.L.J. Sing, Review of selective laser melting: materials and applications, Appl. Phys. Rev. 2 (4) (2015), 041101.
[54] L.E. Murr, S.M. Gaytan, D.A. Ramirez, E. Martinez, J. Hernandez, K.N. Amato, P.W. Shindo, F.R. Medina, R.B.J. Wicker, Metal fabrication by additive manufacturing using laser and electron beam melting technologies, J. Mater. Sci. Technol. 28 (1) (2012) 1–14.
[55] D. Wang, Y. Wang, J. Wang, C. Song, Y. Yang, Z. Zhang, H. Lin, Y. Zhen, S.J. Liao, Design and fabrication of a precision template for spine surgery using selective laser melting (SLM), Materials 9 (7) (2016) 608.
[56] R.J. Van Noort, The future of dental devices is digital, Dent. Mater. 28 (1) (2012) 3–12.
[57] C. Song, Y. Yang, Y. Wang, J.-k. Yu, D.J. Wang, Personalized femoral component design and its direct manufacturing by selective laser melting, Read. Psychol. J. 22 (2) (2016) 330–337.
[58] A.T. Sidambe, Biocompatibility of advanced manufactured titanium implants—a review, Materials 7 (12) (2014) 8168–8188.
[59] B. Vandenbroucke, J.-P.J. Kruth, Selective laser melting of biocompatible metals for rapid manufacturing of medical parts, Read. Psychol. J. 13 (4) (2007) 196–203.
[60] K. Tan, C. Chua, K. Leong, C. Cheah, W. Gui, W. Tan, F.J. Wiria, Engineering, Selective laser sintering of biocompatible polymers for applications in tissue engineering, Bio-Medical. Mater. Eng. 15 (1, 2) (2005) 113–124.
[61] S.H. Ko, H. Pan, C.P. Grigoropoulos, C.K. Luscombe, J.M. Fréchet, D. Poulikakos, All-inkjet-printed flexible electronics fabrication on a polymer substrate by low-temperature high-resolution selective laser sintering of metal nanoparticles, Philos. Soc. Sci. Ed. 18 (34) (2007) 345202.
[62] X. Wang, S. Xu, S. Zhou, W. Xu, M. Leary, P. Choong, M. Qian, M. Brandt, Y. Xie, Topological design and additive manufacturing of porous metals for bone scaffolds and orthopaedic implants: a review, Biomaterials 83 (2016) 127–141.
[63] L. Mullen, R.C. Stamp, W.K. Brooks, E. Jones, C.J. Sutcliffe, Selective Laser Melting: a regular unit cell approach for the manufacture of porous, titanium, bone in-growth constructs, suitable for orthopedic applications, J. Biomed. Mater. Res. Part B: Appl. Biomater. Off. J. Soc. Biomater. The Jpn. Soc. Biomater. Aus. Soc. Biomater. Korean Soc. Biomater. 89 (2) (2009) 325–334.
[64] S.L. Sing, J. An, W.Y. Yeong, F.E.J. Wiria, Laser and electron-beam powder-bed additive manufacturing of metallic implants: a review on processes, materials and designs, J. Orthop. Res. 34 (3) (2016) 369–385.
[65] V. Manakari, G. Parande, M. Gupta, Selective laser melting of magnesium and magnesium alloy powders: A review, Metals 7 (1) (2016) 2.
[66] C.J. Selcuk, Laser metal deposition for powder metallurgy parts, Philos. Med. 54 (2) (2011) 94–99.

[67] M.N. Ahsan, A.J. Pinkerton, R.J. Moat, J.J. Shackleton, A comparative study of laser direct metal deposition characteristics using gas and plasma-atomized Ti–6Al–4V powders, Mater. Sci. Eng. 528 (25–26) (2011) 7648–7657.
[68] C. Leyens, E. Beyer, Innovations in laser cladding and direct laser metal deposition, in: Laser Surface Engineering, Elsevier, 2015, pp. 181–192.
[69] G. Dinda, L. Song, J.J.M. Mazumder, Fabrication of Ti-6Al-4V scaffolds by direct metal deposition, Metall. Mater. Trans. 39 (12) (2008) 2914–2922.
[70] M.N. Ahsan, C.P. Paul, L. Kukreja, A.J.J. Pinkerton, Porous structures fabrication by continuous and pulsed laser metal deposition for biomedical applications; modelling and experimental investigation, J. Mater. Process. Technol. 211 (4) (2011) 602–609.
[71] B.V. Krishna, S. Bose, A.J. Bandyopadhyay, Low stiffness porous Ti structures for load-bearing implants, Acta Biomater. 3 (6) (2007) 997–1006.
[72] W. Xue, B.V. Krishna, A. Bandyopadhyay, S.J. Bose, Processing and biocompatibility evaluation of laser processed porous titanium, Acta Biomater. 3 (6) (2007) 1007–1018.
[73] A. Bandyopadhyay, F. Espana, V.K. Balla, S. Bose, Y. Ohgami, N.M.J. Davies, Influence of porosity on mechanical properties and in vivo response of Ti6Al4V implants, Acta Biomater. 6 (4) (2010) 1640–1648.
[74] G.K. Lewis, E. Schlienger, Design, Practical considerations and capabilities for laser assisted direct metal deposition, Mater. Des. 21 (4) (2000) 417–423.
[75] C. Gao, C. Wang, H. Jin, Z. Wang, Z. Li, C. Shi, Y. Leng, F. Yang, H. Liu, J.J. Wang, Additive manufacturing technique-designed metallic porous implants for clinical application in orthopedics, RSC Adv. 8 (44) (2018) 25210–25227.
[76] L.E. Murr, S.M. Gaytan, E. Martinez, F. Medina, R.B.J. Wicker, Next generation orthopaedic implants by additive manufacturing using electron beam melting, Int. J. Biomater. (2012), 245727, https://doi.org/10.1155/2012/245727, 2012,14 pages.
[77] D. Gu, W. Meiners, K. Wissenbach, R.J. Poprawe, Laser additive manufacturing of metallic components: materials, processes and mechanisms, Int. Mater. Rev. 57 (3) (2012) 133–164.
[78] H. Ali, H. Ghadbeigi, K.J.M.S. Mumtaz, Effect of scanning strategies on residual stress and mechanical properties of Selective Laser Melted Ti6Al4V, Agric. Eng. 712 (2018) 175–187.
[79] T. DebRoy, H. Wei, J. Zuback, T. Mukherjee, J. Elmer, J. Milewski, A.M. Beese, A. Wilson-Heid, A. De, W.J. Zhang, Additive manufacturing of metallic components–process, structure and properties, Prog. Mater. Sci. 92 (2018) 112–224.
[80] D. Herzog, V. Seyda, E. Wycisk, C.J. Emmelmann, Additive manufacturing of metals, Acta Mater. 117 (2016) 371–392.
[81] L.J. Murr, Metallurgy of additive manufacturing: examples from electron beam melting, Acta Mater. 5 (2015) 40–53.
[82] P. Heinl, L. Müller, C. Körner, R.F. Singer, F.A.J. Müller, Cellular Ti–6Al–4V structures with interconnected macro porosity for bone implants fabricated by selective electron beam melting, Acta Biomater. 4 (5) (2008) 1536–1544.
[83] N. Guo, M.C.J. Leu, Additive manufacturing: technology, applications and research needs, Front. Mech. Eng. 8 (3) (2013) 215–243.
[84] S. Al-Bermani, M. Blackmore, W. Zhang, I.J.M. Todd, The origin of microstructural diversity, texture, and mechanical properties in electron beam melted Ti-6Al-4V, Metall. Mater. Trans. 41 (13) (2010) 3422–3434.
[85] K. Amato, S. Gaytan, L. Murr, E. Martinez, P. Shindo, J. Hernandez, S. Collins, F.J. Medina, Microstructures and mechanical behavior of Inconel 718 fabricated by selective laser melting, Acta Mater. 60 (5) (2012) 2229–2239.
[86] K. Mumtaz, N.J. Hopkinson, Selective laser melting of thin wall parts using pulse shaping, J. Mater. Process. Technol. 210 (2) (2010) 279–287.
[87] I. Zergioti, S. Mailis, N. Vainos, C. Fotakis, S. Chen, C.J. Grigoropoulos, Microdeposition of metals by femtosecond excimer laser, Appl. Surf. Sci. 127 (1998) 601–605.
[88] P. Delaporte, A.-P.J. Alloncle, Laser-induced forward transfer: a high resolution additive manufacturing technology, Opt. Laser. Technol. 78 (2016) 33–41.
[89] S. Papazoglou, I.J. Zergioti, Laser Induced Forward Transfer (LIFT) of nano-micro patterns for sensor applications, Microelectron. Eng. 182 (2017) 25–34.
[90] Z. Toth, B. Hopp, T. Szoerenyi, Z. Bor, E.A. Shakhno, V.P. Veiko, in: Pulsed Laser Ablation Mechanisms of Thin Metal Films, Computer-Controlled Microshaping, International Society for Optics and Photonics, 1999, pp. 18–27.
[91] C. Unger, J. Koch, L. Overmeyer, B.N.J. Chichkov, Time-resolved studies of femtosecond-laser induced melt dynamics, Opt. Express 20 (22) (2012) 24864–24872.
[92] T. Sano, H. Yamada, T. Nakayama, I.J. Miyamoto, Experimental investigation of laser induced forward transfer process of metal thin films, Appl. Surf. Sci. 186 (1–4) (2002) 221–226.
[93] A.B. Bullock, P.R.J. Bolton, Laser-induced back ablation of aluminum thin films using picosecond laser pulses, J. Appl. Phys. 85 (1) (1999) 460–465.
[94] L. Hirt, A. Reiser, R. Spolenak, T.J. Zambelli, Additive manufacturing of metal structures at the micrometer scale, Adv. Mater. 29 (17) (2017) 1604211.
[95] M. Zenou, A. Sa'ar, Z. Kotler, Laser transfer of metals and metal alloys for digital microfabrication of 3D objects, Small 11 (33) (2015) 4082–4089.
[96] M. Zenou, A. Sa'Ar, Z.J. Kotler, Laser jetting of femto-liter metal droplets for high resolution 3D printed structures, Sci. Rep. 5 (2015) 17265.
[97] C.W. Visser, R. Pohl, C. Sun, G.W. Römer, B. Huis in 't Veld, D.J. Lohse, Toward 3D printing of pure metals by laser-induced forward transfer, Adv. Mater. 27 (27) (2015) 4087–4092.
[98] M. Xia, J. Sanjayan, Design, Method of formulating geopolymer for 3D printing for construction applications, Mater. Des. 110 (2016) 382–390.
[99] U.M. Dilberoglu, B. Gharehpapagh, U. Yaman, M.J. Dolen, The role of additive manufacturing in the era of industry 4.0, Philos. Med. 11 (2017) 545–554.
[100] A. El-Hajje, E.C. Kolos, J.K. Wang, S. Maleksaeedi, Z. He, F.E. Wiria, C. Choong, A.J.J. Ruys, Physical and mechanical characterisation of 3D-printed porous titanium for biomedical applications, J. Mater. Sci. Mater. Med. 25 (11) (2014) 2471–2480.
[101] D. Banerjee, J.J. Williams, Perspectives on titanium science and technology, Acta Mater. 61 (3) (2013) 844–879.
[102] A.M. Khorasani, M. Goldberg, E.H. Doeven, G.J. Littlefair, Titanium in biomedical applications—properties and fabrication: a review, J. Biomimetics, Biomaterials Tissue Eng. 5 (8) (2015) 593–619.
[103] M.A.-H. Gepreel, M.J. Niinomi, Biocompatibility of Ti-alloys for long-term implantation, J. Mech. Behav. Biomed. Mater. 20 (2013) 407–415.
[104] M.T. Mohammed, Z.A. Khan, A.N.J. Siddiquee, Beta titanium alloys: the lowest elastic modulus for biomedical applications: a review, Int. J. Chem. Mol. Nucl. Mater. Metall. Eng. 8 (8) (2014).
[105] M.J.M.S. Niinomi, Mechanical properties of biomedical titanium alloys, Agric. Eng. 243 (1–2) (1998) 231–236.
[106] L.-C. Zhang, H. Attar, M. Calin, J.J. Eckert, Review on manufacture by selective laser melting and properties of titanium based materials for biomedical applications, Mater. Technol. 31 (2) (2016) 66–76.
[107] L.C. Zhang, H.J. Attar, Selective laser melting of titanium alloys and titanium matrix composites for biomedical applications: a review, Agric. Eng. 18 (4) (2016) 463–475.
[108] X. Tan, Y. Tan, C. Chow, S. Tor, W.J.M.S. Yeong, Metallic powder-bed based 3D printing of cellular scaffolds for orthopaedic implants: a state-of-the-art review on manufacturing, topological design, mechanical properties and biocompatibility, Mater. Sci. Eng. 76 (2017) 1328–1343.
[109] S.A. Yavari, J. van der Stok, Y.C. Chai, R. Wauthle, Z.T. Birgani, P. Habibovic, M. Mulier, J. Schrooten, H. Weinans, A. Zadpoor, Bone regeneration performance of surface-treated porous titanium, Biomaterials 35 (24) (2014) 6172–6181.
[110] Z. Gorgin Karaji, M. Speirs, S. Dadbakhsh, J.-P. Kruth, H. Weinans, A. Zadpoor, S.J. Amin Yavari, Additively manufactured and surface biofunctionalized porous nitinol, ACS Appl. Mater. Interfaces 9 (2) (2017) 1293–1304.
[111] L. Perticarini, G. Zanon, S.M.P. Rossi, F.M.J. Benazzo, Clinical and radiographic outcomes of a trabecular titanium™ acetabular component in hip arthroplasty: results at minimum 5 years follow-up, BMC Muscoskelet. Disord. 16 (1) (2015) 375.
[112] R.F. MacBarb, D.P. Lindsey, S.A. Woods, P.A. Lalor, M.I. Gundanna, S.A.J. Yerby, Fortifying the bone-implant interface part 2: an in vivo evaluation of 3D-printed and TPS-coated triangular implants, Int. J. Spine Surg. 11 (3) (2017) 16.
[113] D.A. Hollander, M. Von Walter, T. Wirtz, R. Sellei, B. Schmidt-Rohlfing, O. Paar, H.-J. Erli, Structural, mechanical and in vitro characterization of individually structured Ti–6Al–4V produced by direct laser forming, J. Biochem. 27 (7) (2006) 955–963.
[114] N. Taniguchi, S. Fujibayashi, M. Takemoto, K. Sasaki, B. Otsuki, T. Nakamura, T. Matsushita, T. Kokubo, S.J.M.S. Matsuda, Effect of pore size on bone ingrowth into porous titanium implants fabricated by additive manufacturing: an in vivo experiment, Mater. Sci. Eng. 59 (2016) 690–701.
[115] B. Wysocki, J. Idaszek, J. Zdunek, K. Rożniatowski, M. Pisarek, A. Yamamoto, W.J. Święszkowski, The influence of selective laser melting (SLM) process parameters on in-vitro cell response, Int. J. Mol. Sci. 19 (6) (2018) 1619.
[116] S. Ponader, E. Vairaktaris, P. Heinl, C.v. Wilmowsky, A. Rottmair, C. Körner, R.F. Singer, S. Holst, K.A. Schlegel, F.W.J. Neukam, Effects of topographical surface modifications of electron beam melted Ti-6Al-4V titanium on human fetal osteoblasts, J. Biomed. Mater. Res. Part A Off. J. Soc. Biomater. Jn. Soc. Biomater. Austr. Soc. Biomater. Korean Soc. Biomater. vol. 84 (4) (2008) 1111–1119.
[117] S. Ponader, C. Von Wilmowsky, M. Widenmayer, R. Lutz, P. Heinl, C. Körner, R.F. Singer, E. Nkenke, F.W. Neukam, K.A. Schlegel, In vivo performance of selective electron beam-melted Ti-6Al-4V structures, J. Biomed. Mater. Res. Part A Off. J. Soc. Biomater. Jn. Soc. Biomater. Austr. Soc. Biomater. Korean Soc. Biomater. vol. 92 (1) (2010) 56–62.
[118] A. Palmquist, A. Snis, L. Emanuelsson, M. Browne, P. Thomsen, Long-term biocompatibility and osseointegration of electron beam melted, free-form–fabricated solid and porous titanium alloy: experimental studies in sheep, J. Biomater. Appl. 27 (8) (2013) 1003–1016.
[119] A.-M. Pobloth, S. Checa, H. Razi, A. Petersen, J.C. Weaver, K. Schmidt-Bleek, M. Windolf, A.Á. Tatai, C.P. Roth, K.-D. Schaser, Mechanobiologically optimized 3D titanium-mesh scaffolds enhance bone regeneration in critical segmental defects in sheep, Sci. Transl. Med. 10 (423) (2018), eaam8828.
[120] A. Gadia, K. Shah, A.J. Nene, Emergence of three-dimensional printing technology and its utility in spine surgery, Asian. J. Spine 12 (2) (2018) 365–371.
[121] J. Imanishi, P.F.J.I. Choong, Three-dimensional printed calcaneal prosthesis following total calcanectomy, Int. J. Surg. Case Rep. 10 (2015) 83–87.
[122] U. Spetzger, A.S.J. Koenig, Individualized three-dimensional printed cage for spinal cervical fusion, Digit. Med. 3 (1) (2017) 1.
[123] T. Punyaratabandhu, B. Lohwongwatana, C. Puncreobutr, A. Kosiyatrakul, P. Veerapan, S.J. Luenam, A patient-matched entire first metacarpal prosthesis in treatment of giant cell tumor of bone, Case. Rep. Orthop. (2017), 4101346, https://doi.org/10.1155/2017/4101346, 2017, 6 pages.
[124] G. Maccauro, P.R. Iommetti, F. Muratori, L. Raffaelli, P.F. Manicone, C.J. Fabbriciani, An overview about biomedical applications of micron and nano size tantalum, Recent Pat. Biotechnol. 3 (3) (2009) 157–165.

[125] V.K. Balla, S. Banerjee, S. Bose, A.J. Bandyopadhyay, Direct laser processing of a tantalum coating on titanium for bone replacement structures, Acta Biomater. 6 (6) (2010) 2329–2334.
[126] J.D. Bobyn, K.-K. Toh, S.A. Hacking, M. Tanzer, J.J.J. Krygier, Tissue response to porous tantalum acetabular cups: a canine model, J. Arthroplast. 14 (3) (1999) 347–354.
[127] J. Bobyn, G. Stackpool, S. Hacking, M. Tanzer, J.J. Krygier, Characteristics of bone ingrowth and interface mechanics of a new porous tantalum biomaterial, J. Bone Jt. Surg. 81 (5) (1999) 907–914.
[128] J.D. Bobyn, R. Poggie, J. Krygier, D. Lewallen, A. Hanssen, R. Lewis, A. Unger, T. O'keefe, M. Christie, S. Nasser, Clinical validation of a structural porous tantalum biomaterial for adult reconstruction, JBJS 86 (suppl_2) (2004) 123–129.
[129] A.F. Kamath, D.G. Lewallen, A.D. Hanssen, Porous tantalum metaphyseal cones for severe tibial bone loss in revision knee arthroplasty: a five to nine-year follow-up, JBJS 97 (3) (2015) 216–223.
[130] V.K. Balla, S. Bodhak, S. Bose, A. Bandyopadhyay, Porous tantalum structures for bone implants: fabrication, mechanical and in vitro biological properties, Acta Biomater. 6 (8) (2010) 3349–3359.
[131] Y. Zhang, X. Zhang, G. Wang, X. Bai, P. Tan, Z. Li, Z. Yu, High strength bulk tantalum with novel gradient structure within a particle fabricated by spark plasma sintering, Mater. Sci. Eng. A 528 (29–30) (2011) 8332–8336.
[132] R. Wauthle, J. Van Der Stok, S.A. Yavari, J. Van Humbeeck, J.-P. Kruth, A.A. Zadpoor, H. Weinans, M. Mulier, J. Schrooten, Additively manufactured porous tantalum implants, Acta Biomater. 14 (2015) 217–225.
[133] L. Thijs, M.L.M. Sistiaga, R. Wauthle, Q. Xie, J.-P. Kruth, J.J. Van Humbeeck, Strong morphological and crystallographic texture and resulting yield strength anisotropy in selective laser melted tantalum, Acta Mater. 61 (12) (2013) 4657–4668.
[134] M. Niinomi, T. Narushima, M. Nakai, Advances in Metallic Biomaterials, Springer, Heidelberg, DE, 2015.
[135] R.W.-W. Hsu, C.-C. Yang, C.-A. Huang, Y.-S. Chen, Electrochemical corrosion studies on Co–Cr–Mo implant alloy in biological solutions, Mater. Chem. Phys. 93 (2–3) (2005) 531–538.
[136] S. Zangeneh, H. Lashgari, A. Roshani, Microstructure and tribological characteristics of aged Co–28Cr–5Mo–0.3 C alloy, Mater. Des. 37 (2012) 292–303.
[137] M. Metikoš-Huković, R. Babić, Passivation and corrosion behaviours of cobalt and cobalt–chromium–molybdenum alloy, Corros. Sci. 49 (9) (2007) 3570–3579.
[138] P. Sinnett-Jones, J. Wharton, R.J. Wood, Micro-abrasion–corrosion of a CoCrMo alloy in simulated artificial hip joint environments, Wear 259 (7–12) (2005) 898–909.
[139] K. Sadiq, R.A. Black, M.J. Stack, Bio-tribocorrosion mechanisms in orthopaedic devices: mapping the micro-abrasion–corrosion behaviour of a simulated CoCrMo hip replacement in calf serum solution, Wear 316 (1–2) (2014) 58–69.
[140] T. Koutsoukis, S. Zinelis, G. Eliades, K. Al-Wazzan, M.A. Rifaiy, Y.S. Al Jabbari, Selective laser melting technique of Co-Cr dental alloys: a review of structure and properties and comparative analysis with other available techniques, J. Prosthodont. 24 (4) (2015) 303–312.
[141] Y. Lu, S. Wu, Y. Gan, J. Li, C. Zhao, D. Zhuo, J.J.M.S. Lin, Investigation on the microstructure, mechanical property and corrosion behavior of the selective laser melted CoCrW alloy for dental application, Mater. Sci. Eng. 49 (2015) 517–525.
[142] F.A. España, V.K. Balla, S. Bose, A.J.M.S. Bandyopadhyay, Design and fabrication of CoCrMo alloy based novel structures for load bearing implants using laser engineered net shaping, Mater. Sci. Eng. 30 (1) (2010) 50–57.
[143] X. Xin, J. Chen, N. Xiang, Y. Gong, B.J. Wei, Surface characteristics and corrosion properties of selective laser melted Co–Cr dental alloy after porcelain firing, Dent. Mater. 30 (3) (2014) 263–270.
[144] Y. Kajima, A. Takaichi, N. Kittikundecha, T. Nakamoto, T. Kimura, N. Nomura, A. Kawasaki, T. Hanawa, H. Takahashi, N. Wakabayashi, Effect of heat-treatment temperature on microstructures and mechanical properties of Co–Cr–Mo alloys fabricated by selective laser melting, Mater. Sci. Eng. 726 (2018) 21–31.
[145] Y. Lu, S. Wu, Y. Gan, S. Zhang, S. Guo, J. Lin, J. Lin, Microstructure, mechanical property and metal release of As-SLM CoCrW alloy under different solution treatment conditions, J. Mech. Behav. Biomed. Mater. 55 (2016) 179–190.
[146] E. Liverani, A. Fortunato, A. Leardini, C. Belvedere, S. Siegler, L. Ceschini, A. Ascari, Fabrication of Co–Cr–Mo endoprosthetic ankle devices by means of Selective Laser Melting (SLM), Mater. Des. 106 (2016) 60–68.
[147] K. Darvish, Z. Chen, M. Phan, T. Pasang, Selective laser melting of Co-29Cr-6Mo alloy with laser power 180–360 W: Cellular growth, intercellular spacing and the related thermal condition, Mater. Char. 135 (2018) 183–191.
[148] Y. Kajima, A. Takaichi, T. Nakamoto, T. Kimura, Y. Yogo, M. Ashida, H. Doi, N. Nomura, H. Takahashi, T. Hanawa, Fatigue strength of Co–Cr–Mo alloy clasps prepared by selective laser melting, J. Mech. Behav. Biomed. Mater. 59 (2016) 446–458.
[149] C. Song, M. Zhang, Y. Yang, D. Wang, Y. Jia-kuo, Morphology and properties of CoCrMo parts fabricated by selective laser melting, Mater. Sci. Eng. 713 (2018) 206–213.
[150] Y.S. Hedberg, B. Qian, Z. Shen, S. Virtanen, I.O. Wallinder, In vitro biocompatibility of CoCrMo dental alloys fabricated by selective laser melting, Dent. Mater. 30 (5) (2014) 525–534.
[151] B. Qian, K. Saeidi, L. Kvetková, F. Lofaj, C. Xiao, Z. Shen, Defects-tolerant Co-Cr-Mo dental alloys prepared by selective laser melting, Dent. Mater. 31 (12) (2015) 1435–1444.
[152] K. Hazlehurst, C.J. Wang, M. Stanford, Evaluation of the stiffness characteristics of square pore CoCrMo cellular structures manufactured using laser melting technology for potential orthopaedic applications, Mater. Design 51 (2013) 949–955.
[153] L. Wang, J. Kang, C. Sun, D. Li, Y. Cao, Z. Jin, Mapping porous microstructures to yield desired mechanical properties for application in 3D printed bone scaffolds and orthopaedic implants, Mater. Design 133 (2017) 62–68.
[154] A.G. Demir, B. Previtali, Additive manufacturing of cardiovascular CoCr stents by selective laser melting, Mater. Design 119 (2017) 338–350.
[155] H. Sahasrabudhe, S. Bose, A. Bandyopadhyay, Laser processed calcium phosphate reinforced CoCrMo for load-bearing applications: processing and wear induced damage evaluation, Acta Biomater. 66 (2018) 118–128.
[156] L. Jauer, W. Meiners, S. Vervoort, C. Gayer, N.A. Zumdick, D. Zander, in: Selective Laser Melting of Magnesium Alloys, European Congress and Exhibition on Powder Metallurgy. European PM Conference Proceedings, The European Powder Metallurgy Association, 2016, pp. 1–6.
[157] D. Zhao, F. Witte, F. Lu, J. Wang, J. Li, L. Qin, Current status on clinical applications of magnesium-based orthopaedic implants: a review from clinical translational perspective, Biomaterials 112 (2017) 287–302.
[158] N. Li, Y. Zheng, Novel magnesium alloys developed for biomedical application: a review, J. Mater. Sci. Technol. 29 (6) (2013) 489–502.
[159] Y. Chen, Z. Xu, C. Smith, J. Sankar, Recent advances on the development of magnesium alloys for biodegradable implants, Acta Biomater. 10 (11) (2014) 4561–4573.
[160] F. Witte, H. Ulrich, C. Palm, E. Willbold, Biodegradable magnesium scaffolds: Part II: peri-implant bone remodeling, J. Biomed. Mater. Res. A 81 (3) (2007) 757–765.
[161] P. Han, P. Cheng, S. Zhang, C. Zhao, J. Ni, Y. Zhang, W. Zhong, P. Hou, X. Zhang, Y. Zheng, In vitro and in vivo studies on the degradation of high-purity Mg (99.99 wt.%) screw with femoral intracondylar fractured rabbit model, Biomaterials 64 (2015) 57–69.
[162] P. Cheng, P. Han, C. Zhao, S. Zhang, H. Wu, J. Ni, P. Hou, Y. Zhang, J. Liu, H. Xu, High-purity magnesium interference screws promote fibrocartilaginous entheses regeneration in the anterior cruciate ligament reconstruction rabbit model via accumulation of BMP-2 and VEGF, Biomaterials 81 (2016) 14–26.
[163] R. Erbel, C. Di Mario, J. Bartunek, J. Bonnier, B. de Bruyne, F.R. Eberli, P. Erne, M. Haude, B. Heublein, M. Horrigan, Temporary scaffolding of coronary arteries with bioabsorbable magnesium stents: a prospective, non-randomised multicentre trial, The Lancet 369 (9576) (2007) 1869–1875.
[164] M. Haude, H. Ince, A. Abizaid, R. Toelg, P.A. Lemos, C. von Birgelen, E.H. Christiansen, W. Wijns, F.-J. Neumann, C. Kaiser, Safety and performance of the second-generation drug-eluting absorbable metal scaffold in patients with de-novo coronary artery lesions (BIOSOLVE-II): 6 month results of a prospective, multicentre, non-randomised, first-in-man trial, The Lancet 387 (10013) (2016) 31–39.
[165] K. Wei, M. Gao, Z. Wang, X. Zeng, Effect of energy input on formability, microstructure and mechanical properties of selective laser melted AZ91D magnesium alloy, Mater. Sci. Eng. 611 (2014) 212–222.
[166] C. Ng, M. Savalani, M. Lau, H. Man, Microstructure and mechanical properties of selective laser melted magnesium, Appl. Surf. Sci. 257 (17) (2011) 7447–7454.
[167] C. Ng, M. Savalani, H. Man, I. Gibson, Layer manufacturing of magnesium and its alloy structures for future applications, Virtual Phys. Prototyp. 5 (1) (2010) 13–19.
[168] C. Shuai, Y. Yang, P. Wu, X. Lin, Y. Liu, Y. Zhou, P. Feng, X. Liu, S. Peng, Laser rapid solidification improves corrosion behavior of Mg-Zn-Zr alloy, J. Alloy. Comp. 691 (2017) 961–969.
[169] A. Singh, S.P. Harimkar, Laser surface engineering of magnesium alloys: a review, Springer 64 (6) (2012) 716–733.
[170] Y. Guan, W. Zhou, H. Zheng, Z. Li, Solidification microstructure of AZ91D Mg alloy after laser surface melting, Appl. Phys. 101 (2) (2010) 339–344.
[171] D.A.M. Holguin, S. Han, N.P. Kim, Magnesium alloy 3D printing by wire and arc additive manufacturing (WAAM), MRS Adv. 3 (49) (2018) 2959–2964.
[172] Y. Li, J. Zhou, P. Pavanram, M. Leeflang, L. Fockaert, B. Pouran, N. Tümer, K.-U. Schröder, J. Mol, H. Weinans, Additively manufactured biodegradable porous magnesium, Acta Biomater. 67 (2018) 378–392.
[173] C. Li, Y. Lai, L. Li, H. Cao, J. Long, X. Wang, L.J. Qin, The in vitro biocompatibility and osteoinductive activity study of magnesium composed PLGA/TCP porous scaffold for bone regeneration, J. Orthop. Trans. 7 (2016) 78.
[174] E. Vorndran, K. Wunder, C. Moseke, I. Biermann, F.A. Müller, K. Zorn, U. Gbureck, Hydraulic setting Mg3 (PO4) 2 powders for 3D printing technology, Adv. Appl. Ceram. 110 (8) (2011) 476–481.
[175] M. Schinhammer, A.C. Hänzi, J.F. Löffler, P. Uggowitzer, Design strategy for biodegradable Fe-based alloys for medical applications, Acta Biomater. 6 (5) (2010) 1705–1713.
[176] T. Kraus, F. Moszner, S. Fischerauer, M. Fiedler, E. Martinelli, J. Eichler, F. Witte, E. Willbold, M. Schinhammer, M. Meischel, Biodegradable Fe-based alloys for use in osteosynthesis: outcome of an in vivo study after 52 weeks, Acta Biomater. 10 (7) (2014) 3346–3353.
[177] H. Hermawan, A. Purnama, D. Dube, J. Couet, D. Mantovani, Fe–Mn alloys for metallic biodegradable stents: degradation and cell viability studies, Acta Biomater. 6 (5) (2010) 1852–1860.
[178] M. Peuster, C. Hesse, T. Schloo, C. Fink, P. Beerbaum, C. von Schnakenburg, Long-term biocompatibility of a corrodible peripheral iron stent in the porcine descending aorta, Biomaterials 27 (28) (2006) 4955–4962.
[179] B. Liu, Y. Zheng, Effects of alloying elements (Mn, Co, Al, W, Sn, B, C and S) on biodegradability and in vitro biocompatibility of pure iron, Acta Biomater. 7 (3) (2011) 1407–1420.
[180] A.V. Do, B. Khorsand, S.M. Geary, A.K. Salem, 3D printing of scaffolds for tissue regeneration applications, Adv. Healthc. Mater. 4 (12) (2015) 1742–1762.
[181] D.-T. Chou, D. Wells, D. Hong, B. Lee, H. Kuhn, P.N. Kumta, Novel processing of iron–manganese alloy-based biomaterials by inkjet 3-D printing, Acta Biomater. 9 (10) (2013) 8593–8603.

[182] D. Hong, D.-T. Chou, O.I. Velikokhatnyi, A. Roy, B. Lee, I. Swink, I. Issaev, H.A. Kuhn, P.N. Kumta, Binder-jetting 3D printing and alloy development of new biodegradable Fe-Mn-Ca/Mg alloys, Acta Biomater. 45 (2016) 375–386.
[183] Y. Li, H. Jahr, K. Lietaert, P. Pavanram, A. Yilmaz, L. Fockaert, M. Leeflang, B. Pouran, Y. Gonzalez-Garcia, H. Weinans, Additively manufactured biodegradable porous iron, Acta Biomater. 77 (2018) 380–393.
[184] J. Zhang, S. Zhao, M. Zhu, Y. Zhu, Y. Zhang, Z. Liu, C.J. Zhang, 3D-printed magnetic Fe 3 O 4/MBG/PCL composite scaffolds with multifunctionality of bone regeneration, local anticancer drug delivery and hyperthermia, J. Mater. Chem. 2 (43) (2014) 7583–7595.
[185] F. Liu, G. Alici, B. Zhang, S. Beirne, W. Li, Structures, Fabrication and characterization of a magnetic micro-actuator based on deformable Fe-doped PDMS artificial cilium using 3D printing, Smart Mater. Struct. 24 (3) (2015), 035015.
[186] K.M. Hambidge, N.F.J.T. Krebs, Zinc deficiency: a special challenge, J. Nutr. 137 (4) (2007) 1101–1105.
[187] B. Hennig, M. Toborek, C.J. McClain, Antiatherogenic properties of zinc: implications in endothelial cell metabolism, Philos. Soc. Sci. Ed. 12 (10) (1996) 711–717.
[188] R. Xiang, D. Ding, L. Fan, X. Huang, K.J.C. Xia, Antibacterial mechanism and safety of zinc oxide, J. Clin. Rehabilitative Tissue Eng. Res. (3) (2014) 470–475.
[189] H. Li, Y. Zheng, L. Qin, Progress of biodegradable metals, Prog. Nat. Sci. Mater. Int. 24 (5) (2014) 414–422.
[190] E. Mostaed, M. Sikora-Jasinska, J.W. Drelich, M. Vedani, Zinc-based alloys for degradable vascular stent applications, Acta Biomater. 71 (2018) 1–23.
[191] S. Zhao, C.T. McNamara, P.K. Bowen, N. Verhun, J.P. Braykovich, J. Goldman, J.W. Drelich, Structural characteristics and in vitro biodegradation of a novel Zn-Li alloy prepared by induction melting and hot rolling, Metall. Mater. Trans. 48 (3) (2017) 1204–1215.
[192] M. Sikora-Jasinska, E. Mostaed, A. Mostaed, R. Beanland, D. Mantovani, M. Vedani, Fabrication, mechanical properties and in vitro degradation behavior of newly developed ZnAg alloys for degradable implant applications, Mater. Sci. Eng. 77 (2017) 1170–1181.
[193] D. Vojtěch, J. Kubásek, J. Šerák, P. Novák, Mechanical and corrosion properties of newly developed biodegradable Zn-based alloys for bone fixation, Acta Biomater. 7 (9) (2011) 3515–3522.
[194] K. Törne, A. Örnberg, J. Weissenrieder, Influence of strain on the corrosion of magnesium alloys and zinc in physiological environments, Acta Biomater. 48 (2017) 541–550.
[195] K. Törne, M. Larsson, A. Norlin, J.J. Weissenrieder, Degradation of zinc in saline solutions, plasma, and whole blood, J. Biomed. Mater. Res. Part B: Appl. Biomater. 104 (6) (2016) 1141–1151.
[196] P.K. Bowen, J. Drelich, J. Goldman, Zinc exhibits ideal physiological corrosion behavior for bioabsorbable stents, Adc. Mater. 25 (18) (2013) 2577–2582.
[197] P.K. Bowen, R.J. Guillory II, E.R. Shearier, J.-M. Seitz, J. Drelich, M. Bocks, F. Zhao, J. Goldman, Metallic zinc exhibits optimal biocompatibility for bioabsorbable endovascular stents, Mater. Sci. Eng. 56 (2015) 467–472.
[198] A.J. Drelich, S. Zhao, R.J. Guillory II, J.W. Drelich, J. Goldman, Long-term surveillance of zinc implant in murine artery: surprisingly steady biocorrosion rate, Acta Biomater. 58 (2017) 539–549.
[199] H. Yang, C. Wang, C. Liu, H. Chen, Y. Wu, J. Han, Z. Jia, W. Lin, D. Zhang, W. Li, Evolution of the degradation mechanism of pure zinc stent in the one-year study of rabbit abdominal aorta model, Biomaterials 145 (2017) 92–105.
[200] A.G. Demir, L. Monguzzi, B. Previtali, Selective laser melting of pure Zn with high density for biodegradable implant manufacturing, Addit. Manuf. 15 (2017) 20–28.
[201] P. Wen, M. Voshage, L. Jauer, Y. Chen, Y. Qin, R. Poprawe, J.H. Schleifenbaum, Laser additive manufacturing of Zn metal parts for biodegradable applications: processing, formation quality and mechanical properties, Mater. Des. 155 (2018) 36–45.
[202] Y. Yu, F. Liu, R. Zhang, J. Liu, Suspension 3D printing of liquid metal into self-healing hydrogel, Adv. Mater. Technol. 2 (11) (2017) 1700173.
[203] I.D. Joshipura, H.R. Ayers, C. Majidi, M.D.J. Dickey, Methods to pattern liquid metals, J. Mater. Chem. 3 (16) (2015) 3834–3841.
[204] L. Yi, J. Liu, Liquid metal biomaterials: a newly emerging area to tackle modern biomedical challenges, Int. Mater. Rev. 62 (7) (2017) 415–440.
[205] J. Liu, L. Yi, Liquid Metal Biomaterials: Principles and Applications, Springer vol. 10 (2018).
[206] F. Liu, Y. Yu, L. Yi, J. Liu, Liquid metal as reconnection agent for peripheral nerve injury, Springer 61 (12) (2016) 939–947.
[207] J. Li, C. Guo, Z. Wang, K. Gao, X. Shi, J. Liu, Electrical stimulation towards melanoma therapy via liquid metal printed electronics on skin, Clin. Transl. Med. 5 (1) (2016) 21.
[208] H. Gui, S. Tan, Q. Wang, Y. Yu, F. Liu, J. Lin, J. Liu, Spraying printing of liquid metal electronics on various clothes to compose wearable functional device, Sci. China Technol. Sci. 60 (2) (2017) 306–316.